J. Plasma Physics (2013), *vol.* 79, *part* 5, *pp.* 893–908. © Cambridge University Press 2013
doi:10.1017/S0022377813000652

Linear and nonlinear obliquely propagating ion-acoustic waves in magnetized negative ion plasma with non-thermal electrons

M. K. MISHRA and S. K. JAIN*
Department of Physics, University of Rajasthan, Jaipur 302004, Rajasthan, India
(mishramukesh105@yahoo.com)

(Received 22 February 2013; revised 17 April 2013; accepted 23 May 2013; first published online 20 June 2013)

Abstract. Ion-acoustic solitons in magnetized low-β plasma consisting of warm adiabatic positive and negative ions and non-thermal electrons have been studied. The reductive perturbation method is used to derive the Korteweg–de Vries (KdV) equation for the system, which admits an obliquely propagating soliton solution. It is found that due to the presence of finite ion temperature there exist two modes of propagation, namely fast and slow ion-acoustic modes. In the case of slow-mode if the ratio of temperature to mass of positive ion species is lower (higher) than the negative ion species, then there exist compressive (rarefactive) ion-acoustic solitons. It is also found that in the case of slow mode, on increasing the non-thermal parameter (γ) the amplitude of the compressive (rarefactive) soliton decreases (increases). In fast ion-acoustic mode the nature and characteristics of solitons depend on negative ion concentration. Numerical investigation in case of fast mode reveals that on increasing γ, the amplitude of compressive (rarefactive) soliton increases (decreases). The width of solitons increases with an increase in non-thermal parameters in both the modes for compressive as well as rarefactive solitons. There exists a value of critical negative ion concentration (α_c), at which both compressive and rarefactive ion-acoustic solitons appear as described by modified KdV soliton. The value of $\alpha_c$decreases with increase in γ.

1. Introduction

Plasmas consisting positive ions, electrons, and significant number of negative ions have been investigated by many authors because of their technological implications in microelectronics (Liberman and Lichtenberg 2005) and plasma science. The multicomponent plasmas having negative ions are found in space environments and laboratory devices (Massey 1976; Gottscho and Gaebe, 1986; Swider 1988; Chaizy et al. 1991; Cooney et al. 1991, 1993; Portnyagain, et al. 1991; Nakamura et al. 2001; Liberman and Lichtenberg 2005). The presence of negative ion plasmas in the Earth's ionosphere in D- and F-regions (Massey 1976; Swider 1988; Portnyagain, et al. 1991) and cometary comae (Chaizy et al. 1991) is now well established. In laboratory, the negative ion plasmas have been observed in plasma processing reactors (Gottscho and Gaebe 1986), low-temperature laboratory experiments (Cooney et al. 1991, 1993; Nakamura et al. 2001; Ichiki et al. 2002), and neutral beam sources (Bacal and Hamilton 1979). In the lower ionosphere (D-region), relatively high-pressure plasma permits the formation of negative ions by attachment of electrons to atoms or molecules.

The negative ions change the plasma potential and the behavior of electrons because of decrease in number of electrons to satisfy the charge neutrality condition. The decrease in the number of electrons reduces the shielding effect, so most of the phenomena are not only affected by the presence of negative ions but also because of the deficiency of electrons. Studies of negative ion plasmas may be applied to understand 'dusty plasmas'. From this perspective, most of the phenomena are actually affected by negative ions as well as lack of electrons.

The observations of the Cassini spacecraft have found heavy negative ions in the upper region of Titan atmosphere (Coates et al. 2007). These particles may act as organic building blocks for even more complicated molecules. The non-thermal electrons are also observed in the low-altitude auroral ionosphere by the auroral particle detector on board the sounding rocket S-310-35 (El-Labany et al. 2000), in low-altitude solar wind by Helios, Cluster, and Ulysses (Stverak et al. 2009), and in solar flare spectra observed by RESIK and RHESSI (Dudik et al. 2011). There are various other observations of energetic electrons/ions in the space, e.g. the Vela satellite has reported the observation of non-thermal ions in the Earth's bow-shock region (Cairns et al. 1995); and the ASPERA on the Phobos 2 satellite has observed loss of energetic ions from the upper

* Teacher research fellow from Government P.G. College, Dholpur 328001,Rajasthan, India.

ionosphere of Mars. The non-thermal electrons/ions are now a common feature of Earth's atmosphere and space plasma (Asbridge et al. 1968; Lundin et al. 1987, 1989; Hall et al. 1991; Dovner et al. 1994; Pillay and Verheest 2005) and have been considered as a component by many authors to explain the nonlinear phenomena such as solitons and double layers observed by the FREJA and Viking satellite.

Theoretically, ion-acoustic Korteweg–de Vries (KdV) solitons were predicted by Washimi and Taniuti (1966). Ion-acoustic solitons were later observed experimentally by Ikezi et al. (1970) using a novel double plasma device. Rarefactive solitons have been observed experimentally in negative ion plasma containing F^- ions (Ludwig et al. 1984; Cooney et al. 1991, 1993; Nakamura et al. 2001). At a critical value of negative ion concentration (α_c), small perturbations are described by the modified KdV (m-KdV) equation and both rarefactive and compressive m-KdV solitons can propagate simultaneously in the same plasma (Saito et al. 1984). The presence of both rarefactive and compressive solitons was confirmed experimentally by Nakamura and Tsukabayashi (1984).

Ion-acoustic solitons in multicomponent, unmagnetized plasma having non-thermal and isothermal electrons with cold ion species were studied by Das and Tagare (1975). Later in the research note, Tagare and Reddy (1987) investigated the effect of ionic temperature on ion-acoustic solitons in a two-ion warm plasma with non-isothermal electrons. In their study Tagare and Reddy (1987) have considered that both ion species have equal temperature. Therefore, their study is limited and cannot be applied when ion species possess different temperatures. While discussing the existence of fast and slow modes, they have claimed that slow mode does not exist in case when the mass ratio of ion species is 1, the result is because of equality of temperature of ion species. Rizzato et al. (1987) studied the temperature effects near critical density of negative ions on ion-acoustic solitons, but did not discuss the slow ion-acoustic mode. Mishra et al. (1994) studied obliquely propagating ion-acoustic solitons in magnetized plasma. Ion-acoustic solitons and double layers in negative ion unmagnetized plasma have been studied by Gill et al. (2004). Fully nonlinear ion-acoustic solitary waves in a plasma with positive–negative ions and non-thermal electrons have been studied by Sabry et al. (2009). In their study they considered cold ion species to derive the Sagdeev potential using pseudo potential formalism. Highly nonlinear ion-acoustic solitary waves in a magnetized warm plasma for a two-component electron–ion plasma using pseudo potential approach have been studied by Barman and Talukdar (2010). Recently, El-labany et al. (2010) studied ion-acoustic double layers in magnetized positive–negative ion plasmas with non-thermal electrons and derived the modified Zakharov–Kuznestov equation. Nonlinear ion-acoustic solitary waves in electronegative plasmas with electrons featuring the Tsallis distribution and cold species of both positive and negative ions have been studied by El-Taibany and Tribeche (2012).

The purpose of the present paper is to study the effect of non-isothermal electrons on linear and nonlinear obliquely propagating ion-acoustic solitary waves in magnetized negative ion plasma. It is found that there exist two modes of ion-acoustic waves, namely slow and fast ion-acoustic modes. The nature of solitons depends on the ratio of temperature to mass of two ion species (σ_1, σ_2, and μ) in case of slow ion-acoustic mode, and in case of fast ion-acoustic mode the negative ion concentration α decides the nature of solitons. It is well known that there are many types of plasmas that can be present in laboratory and space where positive and negative ions coexist. For numerical investigations, we considered (Xe^+, F^-), (Ar^+, F^-), (Cs^+, Cl^-), and (H^+, H^-) plasmas, which are frequently observed in the laboratory and space, e.g. D'Angelo et al. (1966) indicated about the existence of slow and fast modes as early as in 1967 with the (Cs^+, Cl^-) plasma system. Ichiki et al. (2001; 2002) used (Xe^+, F^-) plasma to demonstrate the slow mode ion-acoustic solitons. Cooney et al. (1991, 1993) reported from their experimental observation with (Ar^+, F^-) plasma that presence of negative ion is responsible for the propagation of rarefactive KdV solitons. Moreover, (H^+, H^-) plasma compositions occur in the D- and F-regions of the Earth's ionosphere. Our numerical investigations reveal that slow ion-acoustic mode exists only when ion species possess some finite temperature and ($\sigma_1/\mu \neq \sigma_2$). It is found that in the case of slow mode if ($\sigma_1/\mu < \sigma_2$) then there exist compressive solitons, and for the existence of rarefactive solitons $(\sigma_1/\mu > \sigma_2)$. It is also found that in the case of slow mode, on increasing the non-thermal parameter (γ), the amplitude of compressive (rarefactive) soliton decreases (increases), whereas in the case of fast mode the amplitude of compressive (rarefactive) soliton increases (decreases). It is found that at α_c both compressive and rarefactive solitons exist simultaneously as described by m-KdV solitons. For a given set of parameters, the γ decreases the value of α_c. Effects of strength of magnetic field and angle of obliqueness (θ) on the characteristics of the ion-acoustic solitons have also been studied.

The paper is organized in the following pattern: In Sec. 2 the basic set of equations is given. Derivation of the KdV equation is presented in Sec. 3. In Sec. 4 the m-KdV equation is derived. Section 5 is devoted to result and discussion, and main conclusions have been summarized in Sec. 6.

2. Basic equations

We consider collisionless magnetized plasma consisting of warm adiabatic positive and negative ion species and energetic electrons following Cairn's energy distribution with ($T_e \gg T_{i1}, T_{i2}$) in a uniform external magnetic field $\mathbf{B}_0$ along z- axis. We considered low-β plasma.

The wave is propagating in the (x–z) plane at an angle θ to the external magnetic field $\mathbf{B}_0$. The characteristic

https://doi.org/10.1017/S0022377813000652 Published online by Cambridge University Press

frequency is assumed to be much smaller as compared with the ion–cyclotron frequency.

The nonlinear behavior of ion-acoustic waves in these conditions may be described by the following set of normalized fluid equations:

$$\frac{\partial n_1}{\partial t} + \nabla \cdot (n_1 \mathbf{v}_1) = 0, \tag{1}$$

$$\frac{\partial \mathbf{v_1}}{\partial t} + (\mathbf{v}_1 \cdot \nabla)\, \mathbf{v}_1 = -\frac{1}{\beta_1}\nabla\phi + \frac{\Omega_{i1}}{\omega_{pi}}\mathbf{v}_1 \times \hat{z} - \frac{2\sigma_1}{\beta_1 Z_1}\nabla n_1, \tag{2}$$

$$\frac{\partial n_2}{\partial t} + \nabla \cdot (n_2 \mathbf{v}_2) = 0, \tag{3}$$

$$\frac{\partial \mathbf{v}_2}{\partial t} + (\mathbf{v}_2 \cdot \nabla)\, \mathbf{v}_2 = \frac{\mu\varepsilon_z}{\beta_1}\nabla\phi - \frac{\Omega_{i1}}{\omega_{pi}}\mu\varepsilon_z \mathbf{v}_2 \times \hat{z} - \frac{2\mu\sigma_2}{\beta_1 Z_1}\nabla n_2, \tag{4}$$

$$\nabla^2\phi = n_e - \frac{n_1}{(1-\alpha\varepsilon_z)} + \frac{\alpha\varepsilon_z}{(1-\alpha\varepsilon_z)} n_2. \tag{5}$$

Further, we assume that the characteristic time is very much larger than the electron Larmour period, and length scales are the same in both parallel and perpendicular directions to the magnetic field. Under these conditions the electrons move essentially along the magnetic field (Islam et al. 2009). Therefore, the electron density for energetic electrons following Cairn's distribution is given by Cairns et al. (1996) and El-Labany et al. (2010) as

$$n_e = (1 - \gamma\phi + \gamma\phi^2)e^{\phi}, \tag{6}$$

where

$$\beta_1 = \frac{\left(1 + \alpha\mu\varepsilon_Z^2\right)}{(1-\alpha\varepsilon_Z)}; \quad \alpha = \frac{n_2^{(0)}}{n_1^{(0)}}; \quad \varepsilon_Z = \frac{Z_2}{Z_1}; \quad \mu = \frac{M_1}{M_2};$$

$$\sigma_1 = \frac{T_{i1}}{T_e}; \quad \sigma_2 = \frac{T_{i2}}{T_e}; \quad \Omega_{i1} = \frac{Z_1 e B_0}{M_1 c}.$$

It is worth mentioning that although we assumed the ions to be warm adiabatic, owing to two-dimensional motion, the number of degrees of freedom for this case would be two. Therefore, the value of γ (i.e. the ratio of specific heats) is taken as 2. Here γ is defined as $\gamma = 4\delta/(1+3\delta)$, which reduces to normal isothermal Boltzmann density distribution for $\delta = 0$. Allowing δ to vary from zero to infinity, the value of γ is restricted between $0 \leqslant \gamma < 4/3$. It is to be noted that for larger values of γ the distribution function develops wings for higher velocities and becomes multi-peaked. In the above equations, n_1, $\mathbf{v}_1$ and n_2, $\mathbf{v}_2$ are the density and fluid velocity of the positive and negative ion species, respectively, normalized with respect to their corresponding equilibrium values, namely $n_1^{(0)}$ and $n_2^{(0)}$, and n_e, the electron density, is normalized by $n_e^{(0)}$. Here ϕ is the electrostatic potential, μ is the ratio of the masses of the positive to negative ion species, α is the equilibrium ratio of the density of negative to that of positive ion species, the ratio of temperature of positive ion species to electron temperature is denoted by σ_1 and that of negative ions species by σ_2, and ε_Z is the ratio of the charge multiplicity of the negative to the positive ion species.

In (1)–(5), velocities $(\mathbf{v}_1, \mathbf{v}_2)$, potential (ϕ), time (t), and space coordinate (x) are normalized with respect to ion-acoustic speed in mixture C_s, thermal potential $\frac{T_e}{e}$, inverse of the ion–plasma frequency in the mixture ω_{pi}^{-1}, and the Debye length λ_D respectively. In the mixture, the ion-acoustic speed C_s, the ion–plasma frequency ω_{pi}^{-1}, and the Debye length λ_D are given by

$$C_s = \left[\frac{T_e.\beta_1 Z_1}{M_1}\right]^{1/2}, \quad \omega_{pi}^{-1} = \left[\frac{4\pi n_e^{(0)} e^2 Z_1 \beta_1}{M_1}\right]^{-1/2}$$

$$\text{and} \quad \lambda_D = \left[\frac{T_e}{4\pi n_e^{(0)} e^2}\right]^{1/2}.$$

3. Derivation of the KdV equation

To study the propagation of small-amplitude ion-acoustic waves from the basic set of equations, viz. (1)–(5), we apply weak nonlinear theory, which leads to scaling of coordinates (ξ) and (τ) using stretching as follows:

$$\xi = \varepsilon^{1/2}(\hat{K}.\mathbf{r} - St) \tag{7a}$$

and

$$\tau = \varepsilon^{3/2} t, \tag{7b}$$

where ε is a smallness parameter measuring the weakness of dispersion, S is the phase velocity of the wave to be determined later, $\hat{K}$ is the unit vector along the direction of wave propagation, and

$$\hat{K}.\mathbf{r} = x\sin\theta + z\cos\theta. \tag{7c}$$

Now to balance between nonlinear and dispersive terms, we expand the perturbed quantities n_1, n_2, v_{1z}, v_{2z}, $\mathbf{v}_{1\perp}$, and $\mathbf{v}_{2\perp}$ asymptotically about their equilibrium values in (1)–(5) in powers of ε in the form as

$$\begin{bmatrix} n_1 \\ n_2 \\ v_{1z} \\ v_{2z} \\ \phi \end{bmatrix} = \begin{bmatrix} 1 \\ 1 \\ 0 \\ 0 \\ 0 \end{bmatrix} + \varepsilon \begin{bmatrix} n_1^{(1)} \\ n_2^{(1)} \\ v_{1z}^{(1)} \\ v_{2z}^{(1)} \\ \phi^{(1)} \end{bmatrix} + \varepsilon^2 \begin{bmatrix} n_1^{(2)} \\ n_2^{(2)} \\ v_{1z}^{(2)} \\ v_{2z}^{(2)} \\ \phi^{(2)} \end{bmatrix} + \varepsilon^3 \begin{bmatrix} n_1^{(3)} \\ n_2^{(3)} \\ v_{1z}^{(3)} \\ v_{2z}^{(3)} \\ \phi^{(3)} \end{bmatrix} + \cdots, \tag{8a}$$

$$\begin{bmatrix} \mathbf{v}_{1\perp} \\ \mathbf{v}_{2\perp} \end{bmatrix} = \varepsilon^{3/2} \begin{bmatrix} \mathbf{v}_{1\perp}^{(1)} \\ \mathbf{v}_{2\perp}^{(1)} \end{bmatrix} + \varepsilon^2 \begin{bmatrix} \mathbf{v}_{1\perp}^{(2)} \\ \mathbf{v}_{2\perp}^{(2)} \end{bmatrix} + \varepsilon^{5/2} \begin{bmatrix} \mathbf{v}_{1\perp}^{(3)} \\ \mathbf{v}_{2\perp}^{(3)} \end{bmatrix} + \cdots, \tag{8b}$$

where $\mathbf{v}_{1\perp}$ and $\mathbf{v}_{2\perp}$ represent the perpendicular components of velocities $\mathbf{v}_1$ and $\mathbf{v}_2$ (i.e. in the x and y directions).

Using (7) and (8) in (1)–(5) one can obtain the first-order solutions on equating terms with the same powers of ε. On using the first-order solution, in the Poisson's equation (5), the lowest order, i.e. $O(\varepsilon)$, one gets the

https://doi.org/10.1017/S0022377813000652 Published online by Cambridge University Press

dispersion relation as

$$\frac{Z_1\cos^2\theta}{(1-\alpha\varepsilon_Z)}\left[\frac{1}{\left(\beta_1 Z_1 S^2-2\sigma_1\cos^2\theta\right)}+\frac{\alpha\mu\varepsilon_Z^2}{\left(\beta_1 Z_1 S^2-2\mu\sigma_2\cos^2\theta\right)}\right]=(1-\gamma). \tag{9}$$

Equation (9) is quadratic in S^2, therefore inclusion of a finite ion temperature gives rise to two ion-acoustic modes propagating with different phase velocities, viz.

$$S_{\pm}^2=\left[\left(\frac{1}{2(1-\gamma)}+\frac{(\sigma_1+\mu\sigma_2)}{\beta_1 Z_1}\right)\pm\left\{\left(\frac{1}{2(1-\gamma)}+\frac{(\sigma_1+\mu\sigma_2)}{\beta_1 Z_1}\right)^2-\frac{2\mu}{\beta_1^2 Z_1}\left(\frac{2\sigma_1\sigma_2}{Z_1}+\frac{\left(\sigma_2+\sigma_1\alpha\varepsilon_Z^2\right)}{(1-\gamma)(1-\alpha\varepsilon_Z)}\right)\right\}^{1/2}\right]\cos^2\theta. \tag{10}$$

In (10), (+) sign is corresponding to the fast ion-acoustic mode and (–) sign is for the slow ion-acoustic mode.

On using the first- and second-order solutions, and the next higher order, i.e. $O(\varepsilon^{3/2})$ for continuity equations and z-components of the momentum equations, we get

$$\frac{\partial n_1^{(2)}}{\partial\xi}=\frac{\beta_1 Z_1 S}{\left(\beta_1 Z_1 S^2-2\sigma_1\cos^2\theta\right)}\times\left[\frac{2Z_1\cos^2\theta}{\beta_1 Z_1 S^2-2\sigma_1\cos^2\theta}\frac{\partial\phi^{(1)}}{\partial\tau}+\frac{\omega_{pi}^2}{\Omega_{i1}^2}\frac{Z_1 S^3\sin^2\theta}{\beta_1 Z_1 S^2-2\sigma_1\cos^2\theta}\frac{\partial^3\phi^{(1)}}{\partial\xi^3}+\frac{3Z_1^2 S\cos^4\theta}{\left(\beta_1 Z_1 S^2-2\sigma_1\cos^2\theta\right)^2}\phi^{(1)}\frac{\partial\phi^{(1)}}{\partial\xi}+\frac{\cos^2\theta}{\beta_1 S}\frac{\partial\phi^{(2)}}{\partial\xi}\right], \tag{11}$$

$$\frac{\partial n_2^{(2)}}{\partial\xi}=\frac{\beta_1 Z_1 S}{\left(\beta_1 Z_1 S^2-2\mu\sigma_2\cos^2\theta\right)}\times\left[-\frac{2\mu\varepsilon_z Z_1\cos^2\theta}{\beta_1 Z_1 S^2-2\mu\sigma_2\cos^2\theta}\frac{\partial\phi^{(1)}}{\partial\tau}-\frac{\omega_{pi}^2}{\Omega_{i1}^2}\frac{Z_1 S^3\sin^2\theta}{\mu\varepsilon_z\left(\beta_1 Z_1 S^2-2\mu\sigma_2\cos^2\theta\right)}\frac{\partial^3\phi^{(1)}}{\partial\xi^3}+\frac{3\mu^2\varepsilon_z^2 Z_1^2 S\cos^4\theta}{\left(\beta_1 Z_1 S^2-2\mu\sigma_2\cos^2\theta\right)^2}\phi^{(1)}\frac{\partial\phi^{(1)}}{\partial\xi}-\frac{\mu\varepsilon_z\cos^2\theta}{\beta_1 S}\frac{\partial\phi^{(2)}}{\partial\xi}\right]. \tag{12}$$

Now considering next higher order of the Poisson's equation, i.e. $O(\varepsilon^2)$ gives

$$(1-\gamma)\phi^{(2)}+\frac{\phi^{(1)^2}}{2}-\frac{n_1^{(2)}}{1-\alpha\varepsilon_z}+\frac{\alpha\varepsilon_z n_2^{(2)}}{1-\alpha\varepsilon_z}-\frac{\partial^2\phi^{(1)}}{\partial\xi^2}=0. \tag{13}$$

On differentiating the above equation with respect to ξ and substituting the values from (11) and (12), we get the following KdV equation:

$$\frac{\partial\phi^{(1)}}{\partial\tau}+PQ\phi^{(1)}\frac{\partial\phi^{(1)}}{\partial\xi}+PR\frac{\partial^3\phi^{(1)}}{\partial\xi^3}=0, \tag{14}$$

where coefficients P, Q, and R are given by

$$P=\frac{1-\alpha\varepsilon_z}{\beta_1 Z_1 S\cos^2\theta}\left[\frac{Z_1}{\left(\beta_1 Z_1 S^2-2\sigma_1\cos^2\theta\right)^2}+\frac{\alpha\mu\varepsilon_z^2 Z_1}{\left(\beta_1 Z_1 S^2-2\mu\sigma_2\cos^2\theta\right)^2}\right]^{-1}, \tag{15}$$

$$Q=\left[\frac{3\beta_1 Z_1^3 S^2\cos^4\theta}{2(1-\alpha\varepsilon_z)}\left\{\frac{1}{\left(\beta_1 Z_1 S^2-2\sigma_1\cos^2\theta\right)^3}-\frac{\alpha\mu^2\varepsilon_z^3}{\left(\beta_1 Z_1 S^2-2\mu\sigma_2\cos^2\theta\right)^3}\right\}-\frac{1}{2}\right], \tag{16}$$

$$R=\frac{1}{2}+\frac{\omega_{pi}^2}{\Omega_{i1}^2}\frac{\beta_1 Z_1^2 S^4\sin^2\theta}{2(1-\alpha\varepsilon_z)}\left[\frac{1}{\left(\beta_1 Z_1 S^2-2\sigma_1\cos^2\theta\right)^2}+\frac{\alpha}{\mu}\frac{1}{\left(\beta_1 Z_1 S^2-2\mu\sigma_2\cos^2\theta\right)^2}\right]. \tag{17}$$

The stationary solitary wave solution of the nonlinear KdV equation (14) in a moving frame with velocity u using the standard transformation $\eta=\xi-u\tau$ under appropriate boundary conditions, viz. $\phi^{(1)}\to 0$, $d\phi^{(1)}/d\eta\to 0$, $d^2\phi^{(1)}/d\eta^2\to 0$ as $\eta\to\pm\infty$ may be given by (Yadav and Sharma 1990)

$$\phi=\phi_m\sec h^2[\delta^{-1}(\xi-u\tau)], \tag{18}$$

where ϕ is used in place of $\phi^{(1)}$ for brevity and convenience, and amplitude ϕ_m and width δ are given by ${}^{3u}/_{PQ}$ and $2(PR/u)^{1/2}$ respectively. Here amplitude ϕ_m and width δ are functions of various plasma parameters. It can be seen that the nature of solitary wave depends on coefficient PQ, and the positive and negative values of the coefficient PQ will be associated with positive (compressive) and negative (rarefactive) solitary waves. It is found that the criteria for compressive and rarefactive solitary waves depend on temperatures and masses of positive and negative ion species.

From (10), for slow ion-acoustic mode, if the ions are considered to be cold, i.e. $(\sigma_1=\sigma_2=0)$, the value of phase velocity in slow mode (S_-) turns out to be 0, therefore there is no existence of slow ion-acoustic mode. The slow mode also does not exist when $(\sigma_1/\mu=\sigma_2)$. Therefore, it may be concluded that for the existence of slow mode, $(\sigma_1/\mu\neq\sigma_2)$ with non-zero values of σ_1 and σ_2.

In the case of fast mode it is found that α is a significant parameter to decide the nature of ion-acoustic solitons. It is to be noted that there exists α_c at which coefficient Q of the KdV equation vanishes, therefore the KdV equation is no longer valid to study soliton solution at α_c. To study fast ion-acoustic soliton at α_c, we have to go for the m-KdV equation.

4. Derivation of the m-KdV equation

To derive the m-KdV equation, we used the same stretching for co-ordinates and time, viz. (7) as applied in the KdV equation and employ a different perturbation expansion for the dependent quantities to derive appropriate equation,

$$\begin{bmatrix} n_1 \\ n_2 \\ v_{1z} \\ v_{2z} \\ \phi \end{bmatrix} = \begin{bmatrix} 1 \\ 1 \\ 0 \\ 0 \\ 0 \end{bmatrix} + \varepsilon^{\frac{1}{2}} \begin{bmatrix} n_1^{(1)} \\ n_2^{(1)} \\ v_{1z}^{(1)} \\ v_{2z}^{(1)} \\ \phi^{(1)} \end{bmatrix} + \varepsilon^{1} \begin{bmatrix} n_1^{(2)} \\ n_2^{(2)} \\ v_{1z}^{(2)} \\ v_{2z}^{(2)} \\ \phi^{(2)} \end{bmatrix} + \varepsilon^{\frac{3}{2}} \begin{bmatrix} n_1^{(3)} \\ n_2^{(3)} \\ v_{1z}^{(3)} \\ v_{2z}^{(3)} \\ \phi^{(3)} \end{bmatrix} + \dots \tag{19a}$$

$$\begin{bmatrix} \mathbf{v}_{1x,y} \\ \mathbf{v}_{2x,y} \end{bmatrix} = \varepsilon \begin{bmatrix} \mathbf{v}_{1x,y}^{(1)} \\ \mathbf{v}_{2x,y}^{(1)} \end{bmatrix} + \varepsilon^{\frac{3}{2}} \begin{bmatrix} \mathbf{v}_{1x,y}^{(2)} \\ \mathbf{v}_{2x,y}^{(2)} \end{bmatrix} + \varepsilon^{2} \begin{bmatrix} \mathbf{v}_{1x,y}^{(3)} \\ \mathbf{v}_{2x,y}^{(3)} \end{bmatrix} + \dots \tag{19b}$$

By employing expansion (19) and on equating the terms of the same power in ε, we obtain a set of equations in different order of ε.

Now the Poisson's equation (13) at $O(\varepsilon^2)$ gives the following:

$$(1-\gamma)\phi^{(2)} + \frac{1}{2}\phi^{(1)^2} - \frac{n_1^{(2)}}{(1-\alpha\varepsilon_z)} + \frac{\alpha\varepsilon_z n_2^{(2)}}{(1-\alpha\varepsilon_z)} = 0. \tag{20}$$

On substituting the values of $n_1^{(2)}$and $n_2^{(2)}$ from the second-order solutions,

$$\left[\frac{3\beta_1 Z_1^3 S^2 \cos^4\theta}{2(1-\alpha\varepsilon_z)}\left\{\frac{1}{\left(\beta_1 Z_1 S^2 - 2\sigma_1\cos^2\theta\right)^3} - \frac{\alpha\mu^2\varepsilon_z^3}{\left(\beta_1 Z_1 S^2 - 2\mu\sigma_2\cos^2\theta\right)^3}\right\} - \frac{1}{2}\right]\phi^{(1)^2} = 0, \tag{21}$$

$$Q\phi^{(1)^2} = 0. \tag{22}$$

It is clear that the above equation is satisfied identically owing to the criticality condition (i.e. $Q = 0$).

Now considering the next higher order, i.e. $O(\varepsilon^2)$, for the continuity equations and the z-components of momentum equations, and using the first- and second-order solutions,

$$\frac{\partial n_1^{(3)}}{\partial\xi} = \frac{\beta_1 Z_1 S}{(\beta_1 Z_1 S^2 - 2\sigma_1\cos^2\theta)} \times \left[\begin{aligned} &\frac{2Z_1\cos^2\theta}{(\beta_1 Z_1 S^2 - 2\sigma_1\cos^2\theta)}\frac{\partial\phi^{(1)}}{\partial\tau} + \frac{\omega_{pi}^2}{\Omega_{i1}^2}\frac{Z_1 S^3\sin^2\theta}{(\beta_1 Z_1 S^2 - 2\sigma_1\cos^2\theta)}\frac{\partial^3\phi^{(1)}}{\partial\xi^3} \\ &+\frac{3Z_1^2 S\cos^4\theta}{(\beta_1 Z_1 S^2 - 2\sigma_1\cos^2\theta)^2}\frac{\partial}{\partial\xi}\left(\phi^{(1)}\phi^{(2)}\right) + \frac{\cos^2\theta}{\beta_1 S}\frac{\partial\phi^{(3)}}{\partial\xi} \\ &+\frac{3Z_1^3 S\cos^6\theta}{(\beta_1 Z_1 S^2 - 2\sigma_1\cos^2\theta)}\left\{\frac{9\beta_1 Z_1 S^2}{2(\beta_1 Z_1 S^2 - 2\sigma_1\cos^2\theta)} - 2\right\}\phi^{(1)^2}\frac{\partial\phi^{(1)}}{\partial\xi} \end{aligned}\right], \tag{23}$$

$$\frac{\partial n_2^{(3)}}{\partial\xi} = \frac{\beta_1 Z_1 S}{(\beta_1 Z_1 S^2 - 2\mu\sigma_2\cos^2\theta)} \times \left[\begin{aligned} &-\frac{2\mu\varepsilon_Z Z_1\cos^2\theta}{(\beta_1 Z_1 S^2 - 2\mu\sigma_2\cos^2\theta)}\frac{\partial\phi^{(1)}}{\partial\tau} - \frac{\omega_{pi}^2}{\Omega_{i1}^2}\frac{1}{\mu\varepsilon_Z}\frac{Z_1 S^3\sin^2\theta}{(\beta_1 Z_1 S^2 - 2\mu\sigma_2\cos^2\theta)}\frac{\partial^3\phi^{(1)}}{\partial\xi^3} \\ &+\frac{3\mu^2\varepsilon_Z^2 Z_1^2 S\cos^4\theta}{(\beta_1 Z_1 S^2 - 2\mu\sigma_2\cos^2\theta)^2}\frac{\partial}{\partial\xi}\left(\phi^{(1)}\phi^{(2)}\right) - \frac{\mu\varepsilon_Z\cos^2\theta}{\beta_1 S}\frac{\partial\phi^{(3)}}{\partial\xi} \\ &-\frac{3\mu^2\varepsilon_Z^2 Z_1^2 S\cos^6\theta}{(\beta_1 Z_1 S^2 - 2\mu\sigma_2\cos^2\theta)}\left\{\frac{9\beta_1\varepsilon_Z Z_1 S^2}{2(\beta_1 Z_1 S^2 - 2\mu\sigma_2\cos^2\theta)} - 2\right\}\phi^{(1)^2}\frac{\partial\phi^{(1)}}{\partial\xi} \end{aligned}\right]. \tag{24}$$

Now taking the next order Poisson's equation, i.e. $O(\varepsilon^{3/2})$,

$$\frac{\partial^2\phi^{(1)}}{\partial\xi^2} - (1-\gamma)\phi^{(3)} - \phi^{(1)}\phi^{(2)} - \frac{(1+3\beta)}{6}\phi^{(1)^3} + \frac{n_1^{(3)}}{(1-\alpha\varepsilon_Z)} - \frac{\alpha\varepsilon_Z n_2^{(3)}}{(1-\alpha\varepsilon_Z)} = 0. \tag{25}$$

Differentiating (25) w.r.t. ξ and substituting the values from (23) and (24), we get the m-KdV equation in the following form (Watanabe 1984):

$$\frac{\partial\phi^{(1)}}{\partial\tau} + PM\phi^{(1)^2}\frac{\partial\phi^{(1)}}{\partial\xi} + PR\frac{\partial^3\phi^{(1)}}{\partial\xi^3} = 0. \tag{26}$$

Here the coefficients of the m-KdV equation P and R are given by (15) and (17), and M as

$$\begin{aligned} M = &\frac{1}{(1-\alpha\varepsilon_Z)}\frac{3\beta_1 Z_1^4 S^2\cos^6\theta}{2\left(\beta_1 Z_1 S^2 - 2\sigma_1\cos^2\theta\right)^4} \\ &\times\left[\frac{9\beta_1 Z_1 S^2}{4\left(\beta_1 Z_1 S^2 - 2\sigma_1\cos^2\theta\right)} - 1\right] \\ &+\frac{1}{(1-\alpha\varepsilon_Z)}\frac{3\beta_1\alpha\mu^3\varepsilon_Z^3 Z_1^3 S^2\cos^6\theta}{2\left(\beta_1 Z_1 S^2 - 2\mu\sigma_2\cos^2\theta\right)^4} \\ &\times\left[\frac{9\beta_1\varepsilon_Z Z_1 S^2}{4\left(\beta_1 Z_1 S^2 - 2\mu\sigma_2\cos^2\theta\right)} - 1\right] - \frac{(1+3\beta)}{4}. \end{aligned} \tag{27}$$

For the steady state solution of the m-KdV equation (26), using the same transformations as used for the KdV soliton under appropriate boundary conditions,

https://doi.org/10.1017/S0022377813000652 Published online by Cambridge University Press

the soliton solution in case of the m-KdVequation is

$$\frac{1}{2}\left(\frac{d\phi}{d\eta}\right)^2 + \psi(\phi) = 0, \tag{28}$$

where $\psi(\phi)$ is the Sagdeev potential given by

$$\psi(\phi) = \frac{1}{PR}\left(\frac{1}{12}PM\phi^4 - \frac{1}{2}u\phi^2\right). \tag{29}$$

The soliton solution of (26) is given by

$$\phi = \phi_m \sec h[\delta^{-1}(\xi - u\tau)]. \tag{30}$$

Here the amplitude and width of m-KdV solitons are given by $\phi_m = \pm(6u/PM)^{1/2}$ and $\delta = (PR/u)^{1/2}$ respectively.

5. Result and discussion

5.1. Slow ion-acoustic mode

The phase velocity given by (10) shows that there exist two wave mode propagations in such a system having different phase velocities by considering positive and negative signs between the two terms of (10), namely fast and slow ion-acoustic modes. Here we found that two modes exist only when at least one ion species possesses finite temperature. If the two ion species possess some finite temperature with the temperature to mass ratio of both positive and negative ion species equal to $(\sigma_1/\mu = \sigma_2)$, then the slow ion-acoustic mode does not exist. It is found that for the existence of the slow mode $(\sigma_1/\mu \neq \sigma_2)$. It is also found that for the existence of slow ion-acoustic compressive solitons, $(\sigma_1/\mu < \sigma_2)$, and for $(\sigma_1/\mu > \sigma_2)$ there exist only rarefactive solitons. Therefore, we conclude that the masses and temperatures of two ion species are the parameters to decide the nature of ion-acoustic solitons in case of slow mode.

We have done numerical calculation for the amplitude of four different plasma systems. Our plasma model is inspired by the experimental studies of Ichiki et al. (2001; 2002). They studied the propagation of ion-acoustic waves in (Xe^+, F^-) and (Ar^+, F^-) plasmas. In the present study we considered (H^+, H^-), (Ar^+, F^-), (Cs^+, Cl^-), and (Xe^+, F^-) plasmas in the presence of non-thermal electrons. The mass ratio for these plasma systems (i.e. $\mu = m_1/m_2$) are 1, 2.1, 3.75, and 6.667 respectively. For the actual existence of the slow ion-acoustic mode, the phase velocity (S_-) of the slow ion-acoustic mode must be greater than the thermal velocity of ions. In such a case, the Landau damping will be small and therefore the wave will not Landau damp. If we consider positive ions at lower temperature such that $(\sigma_1/\mu < \sigma_2)$ than negative ions, there exist compressive solitons, and if the temperature of negative ions is lower than that of positive ion species such that $(\sigma_1/\mu > \sigma_2)$, then there exist rarefactive solitons. The results obtained by our numerical calculation show that for the (Xe^+, F^-) plasma system having $(\sigma_1, \sigma_2) =$ (0.001, 0.1) and α lying in the range of (0.1–0.9), the ratio of phase velocities to the ions thermal velocity lies in the range of (23.6–10.5). The above discussion clearly shows that in the case of slow ion-acoustic mode the mass and temperature ratios of the ion species with electron temperature are significant parameters. The experimental observations of the slow ion-acoustic mode also show that the mass ratios of ion species and electron temperature are relevant parameters for the existence of slow mode.

In Fig. 1 the variation of amplitude with α for four different plasma systems (i.e. (H^+, H^-), (Ar^+, F^-), (Cs^+, Cl^-), and (Xe^+, F^-)) with two sets of different temperature parameters has been shown. It is found that for $(\sigma_1, \sigma_2) = (0, 0.1)$ there exists compressive soliton, while for $(\sigma_1, \sigma_2) = (0.1, 0)$ there exists rarefactive soliton. We calculated the phase velocity of the slow mode, and thermal velocities of ion species and found that the ratio of phase velocity to thermal velocity of positive ion lies in the range of (23.6–13.3) in case of compressive solitons, and in case of rarefactive solitons the ratio of phase velocity to thermal velocity of negative ions lies in the range of (15.4–10.46). As the phase velocities of ions depend on temperature and mass of ion species, to find out the effect of mass ratio for the fixed values of (σ_1, σ_2), we found from Fig. 1 that the amplitude of compressive (rarefactive) solitons increases (decreases) with μ, that is, larger the mass ratio of positive to negative ion species, larger (smaller) the amplitude in case of compressive (rarefactive) solitons. It is also found that the amplitude of compressive and rarefactive solitons increases with an increase in α.

We considered the (Xe^+, F^-) plasma system in which the slow ion-acoustic mode dominates. To find out the effect of γ on the amplitude of compressive solitons, our numerical calculations show that an increase in γ decreases (increases) the amplitude of compressive (rarefactive) soliton. An increase in γ increases energetic electrons in the system, which raises the frequency of ion oscillation, leading to enhanced phase velocity of waves. Hence, the soliton propagates with higher speed and the amplitude of rarefactive ion-acoustic solitons increases, whereas in case of compressive solitons the phase velocity of soliton diminishes, so the amplitude of compressive soliton also decreases. In Fig. 2 the variation of amplitude with α for three different negative ion temperature (σ_2), keeping positive ion temperature ratio (σ_1) as constant for compressive solitary waves has been shown. It is found that an increase in the value of σ_2 increases the amplitude of compressive soliton owing to increase in thermal speed of negative ion on increasing the negative ion temperature. It can be seen that in the case of rarefactive solitary waves keeping the value of σ_2 constant, an increase in the temperature ratio of positive ion species (σ_1), the thermal speed of positive ion enhances, and due to enhancement in the thermal speed of positive ions the amplitude of the ion-acoustic rarefactive soliton increases. In Figs. 3 and 4 the variation of amplitude with θ in an external magnetic

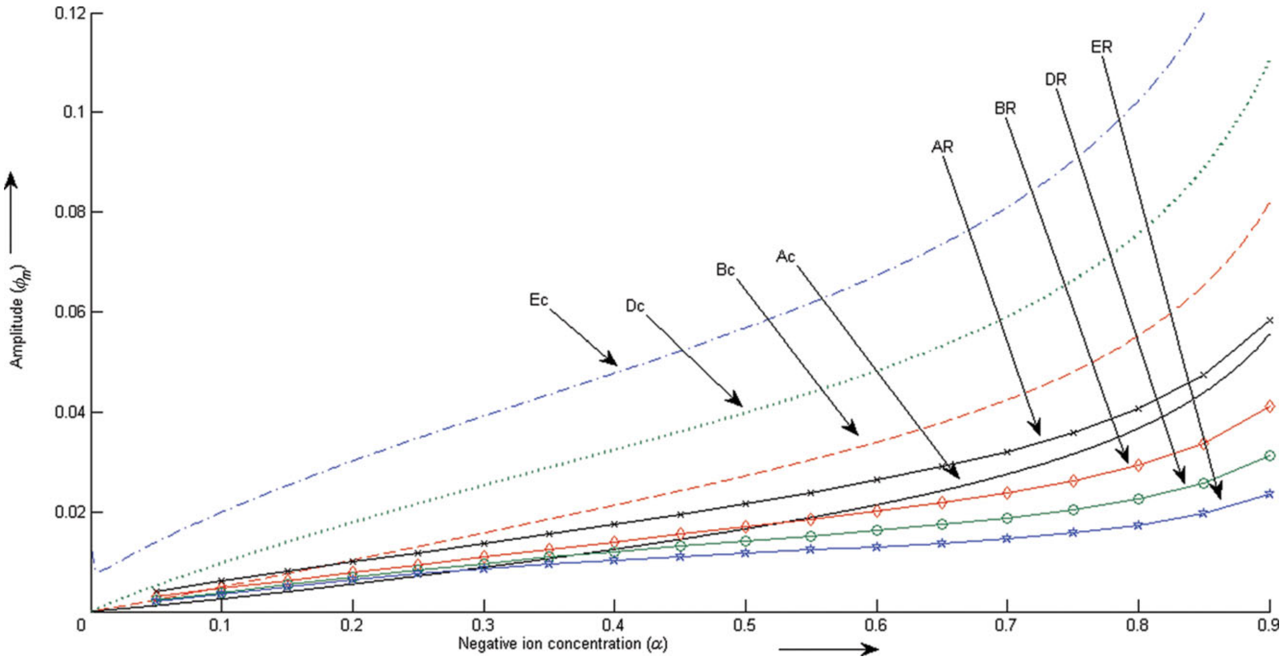

Figure 1. (Colour online) Variation of the slow ion-acoustic soliton amplitude $|\phi_m|$ with negative ion concentration (α) for (H^+, H^-), (Ar^+, F^-), (Cs^+, Cl^-), and (Xe^+, F^-) plasma systems with plasma parameters as ($Z_1 = 1, Z_2 = 1$, $\varepsilon_Z = 1$, $\sigma_1 = 0, \sigma_2 = 0.1, \theta = 15^0, \gamma = 0.25$ $(\omega_{pi}/\Omega_i) = 5$, and $u = 0.02$) considering ($\mu = 1.0$ (solid line A_C), 2.1 (dashed line B_C), 3.75 (dotted line D_C), and 6.667 (dot dashed line E_C)) for compressive solitons and with ($\sigma_1 = 0.1, \sigma_2 = 0$) keeping all other parameters fixed for the rarefactive solitons represented by($\mu = 1.0$ (solid line with AR), 2.1(solid line with BR), 3.75 (solid line with DR), and 6.667 (solid line with ER)).

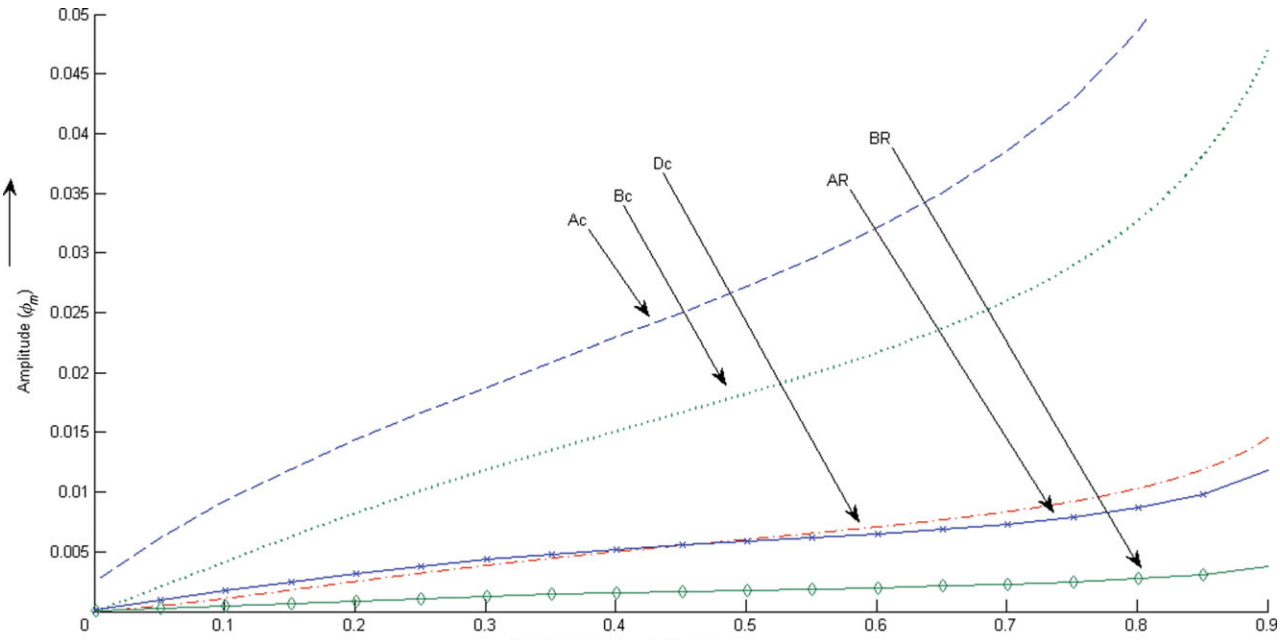

Figure 2. (Colour online) Variation of the slow ion-acoustic soliton amplitude $|\phi_m|$ with negative ion concentration (α) for (Xe^+, F^-) plasma system with plasma parameters as ($Z_1 = 1, Z_2 = 1$, $\varepsilon_Z = 1$, $\sigma_1 = 0, \sigma_2 = 0.1, \theta = 15^0, \gamma = 0.25$, $(\omega_{pi}/\Omega_i) = 5$, $u = 0.02$, and $\mu = 6.667$) at different values of σ_1 and σ_2. Curves A_C, B_C, and D_C refer to compressive solitons and AR and BR refer to rarefactive solitons for five sets of $(\sigma_1, \sigma_2) = (0.01, 0.1)$ shown by dashed line, (0.01, 0.05) shown by dotted line, (0.01, 0.01) shown by dot dashed line, (0.1, 0.01) shown by solid line with ★, and (0.05, 0.01) shown by solid line with ◇ respectively.

field has been shown for three different values of γ. It is found that the amplitude of compressive as well as rarefactive solitons increases with θ. The amplitude increases slowly for smaller angles, but for larger values of θ the amplitude of the soliton increases sharply. It is to be noted that the amplitude of compressive (rarefactive) soliton decreases (increases) with increase in γ.

The numerical calculation of width of soliton reveals that the width of compressive and rarefactive solitons

https://doi.org/10.1017/S0022377813000652 Published online by Cambridge University Press

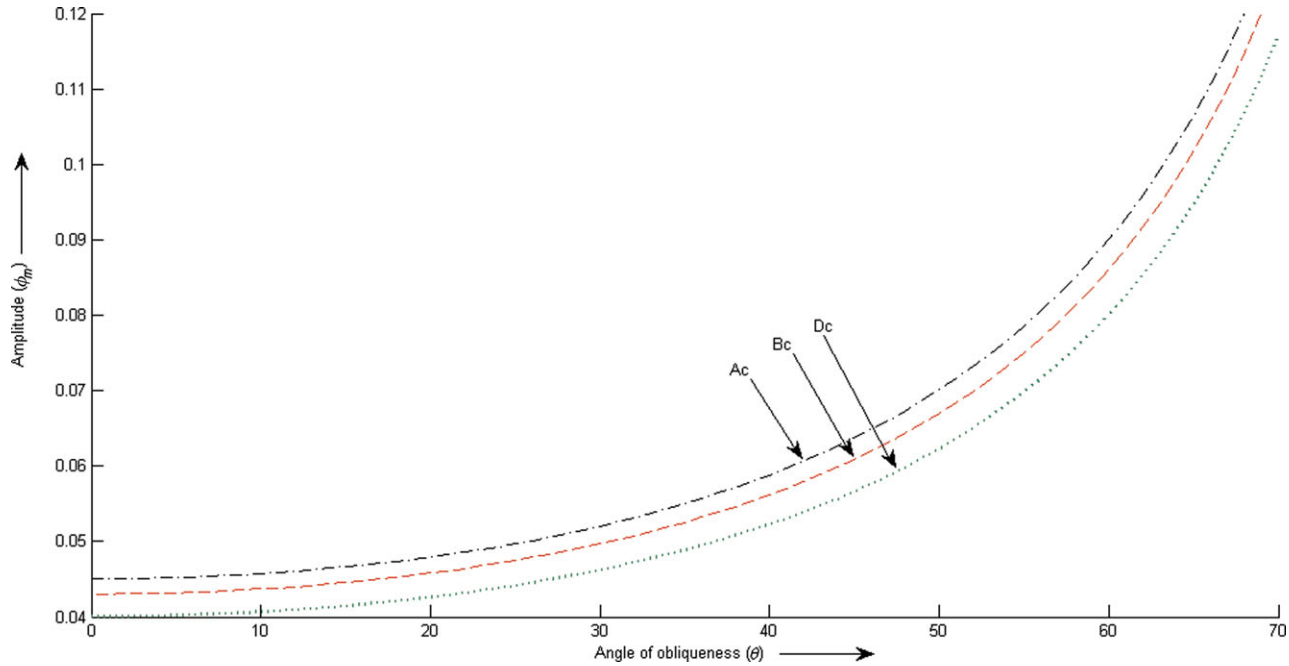

Figure 3. (Colour online) Variation of the slow ion-acoustic soliton amplitude $|\phi_m|$ with angle of obliqueness (θ) for compressive solitons for (Xe^+, F^-) plasma system with plasma parameters as ($Z_1 = 1, Z_2 = 1$, $\varepsilon_Z = 1$, $\sigma_1 = 0, \sigma_2 = 0.1, \alpha = 0.2$, $(\omega_{pi}/\Omega_i) = 5$, $u = 0.03$, and $\mu = 6.667$) for three different values of non-thermal parameter ($\gamma = 0$ (shown by dot dashed line), 0.15 (shown by dotted line), and 0.35 (shown by dotted line).

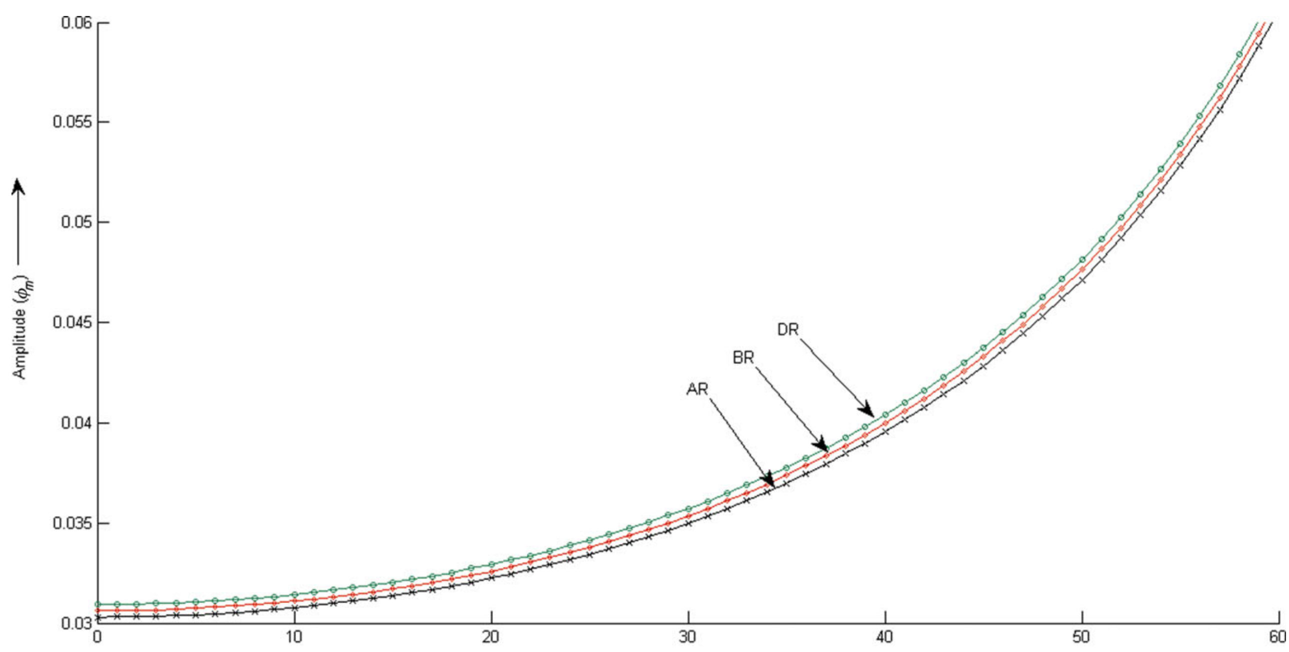

Figure 4. (Colour online) Variation of the slow ion-acoustic soliton amplitude $|\phi_m|$ with angle of obliqueness (θ) for rarefactive solitons for (Xe^+, F^-) plasma system with plasma parameters as ($Z_1 = 1, Z_2 = 1$, $\varepsilon_Z = 1$, $\sigma_1 = 0.1, \sigma_2 = 0, \alpha = 0.2$, $\left(\omega_{pi}/\Omega_i\right) = 5$, $u = 0.03$, and $\mu = 6.667$) for three different values of non-thermal parameter ($\gamma = 0$ (shown by solid line with AR), 0.2 (shown by solid line with BR), and 0.4 (shown by solid line with DR)).

increases with increase in θ, and reaches peak near $\theta \sim 53^0$, but on further increase in obliqueness the width decreases continuously. Figures 5 and 6 show the variation of width with θ for three different values of γ. It is found that the width is higher for higher values of γ for both compressive and rarefactive solitons. In Fig. 7, the variation in width of compressive soliton with strength of magnetic field for three different values of γ has been plotted. It is to be noted that width of the soliton increases slowly with increase in magnetic field, and for higher strength of magnetic field, width increases sharply. It is also found that width of the

https://doi.org/10.1017/S0022377813000652 Published online by Cambridge University Press

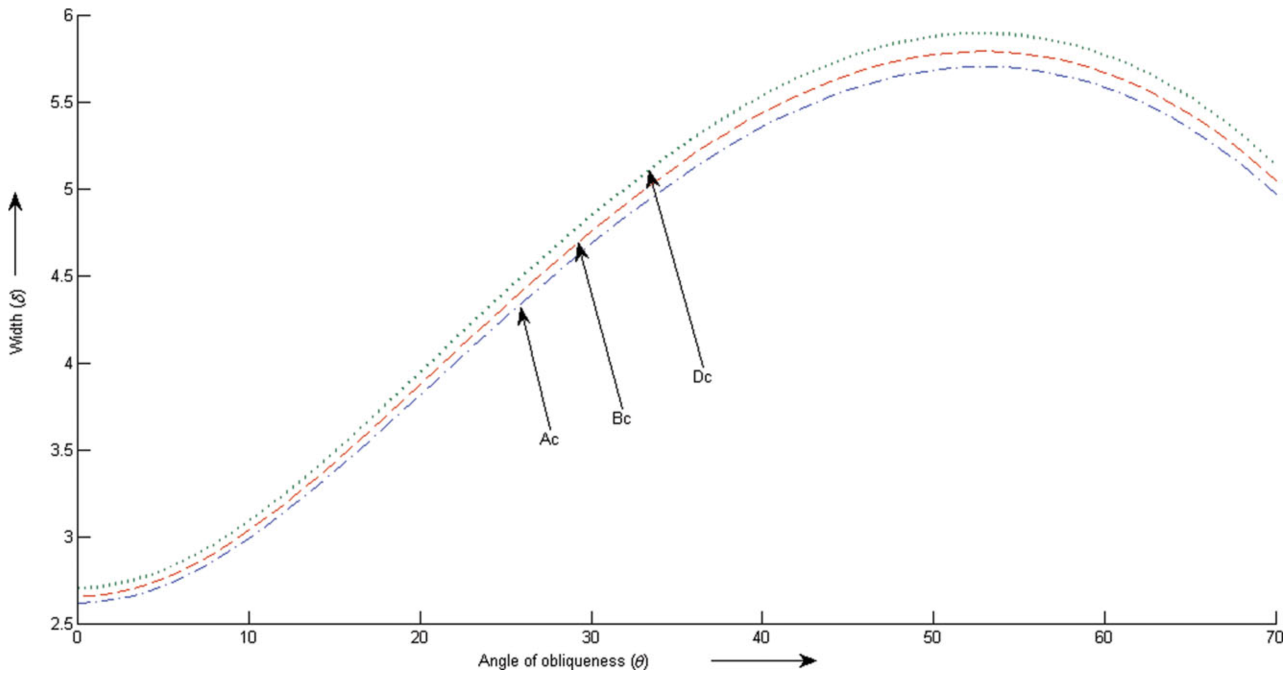

Figure 5. (Colour online) Variation of the slow ion-acoustic soliton width δ with angle of obliqueness (θ) for compressive solitons for (Xe^{+}, F^{-}) plasma system with plasma parameters as ($Z_1 = 1, Z_2 = 1$, $\varepsilon_Z = 1$, $\sigma_1 = 0, \sigma_2 = 0.1, \alpha = 0.2$, $(\omega_{pi}/\Omega_i) = 5$, $u = 0.03$, and $\mu = 6.667$) for three different values of non-thermal parameter ($\gamma = 0$ (shown by dot dashed line), 0.15 (shown by dotted line), and 0.35 (shown by dotted line)).

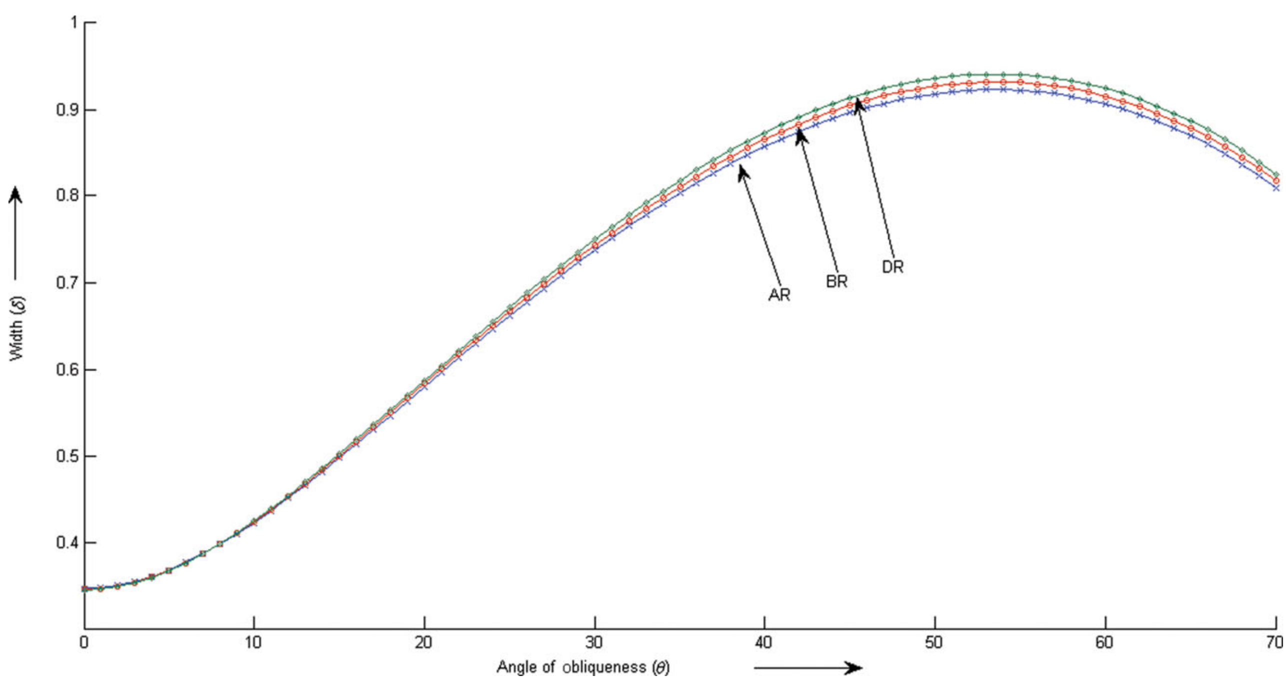

Figure 6. (Colour online) Variation of the slow ion-acoustic soliton width δ with angle of obliqueness (θ) for rarefactive solitons for (Xe^{+}, F^{-}) plasma system with plasma parameters as ($Z_1 = 1, Z_2 = 1$, $\varepsilon_Z = 1$, $\sigma_1 = 0.1, \sigma_2 = 0$, $\alpha = 0.2$, $\left(\omega_{pi}/\Omega_i\right) = 5$, $u = 0.03$, and $\mu = 6.667$) for three different values of non-thermal parameter ($\gamma = 0$ (shown by solid line AR) with 0.2 (shown by solid line with BR), and 0.4 (shown by solid line with DR)).

soliton in both the cases of compressive and rarefactive solitons increases with γ.

5.2. Fast ion-acoustic mode

For our discussion of fast mode solitary waves, we numerically evaluated the amplitude by using phase velocity S_+ from (10) for different plasma systems, namely (H^{+}, H^{-}), (Ar^{+}, F^{-}), (Cs^{+}, Cl^{-}), and (Xe^{+}, F^{-}). It is found that both compressive and rarefactive solitons exist depending on the concentration of negative ion in the plasma system. For the existence of fast ion-acoustic mode, the phase velocity of the fast ion-acoustic mode

https://doi.org/10.1017/S0022377813000652 Published online by Cambridge University Press

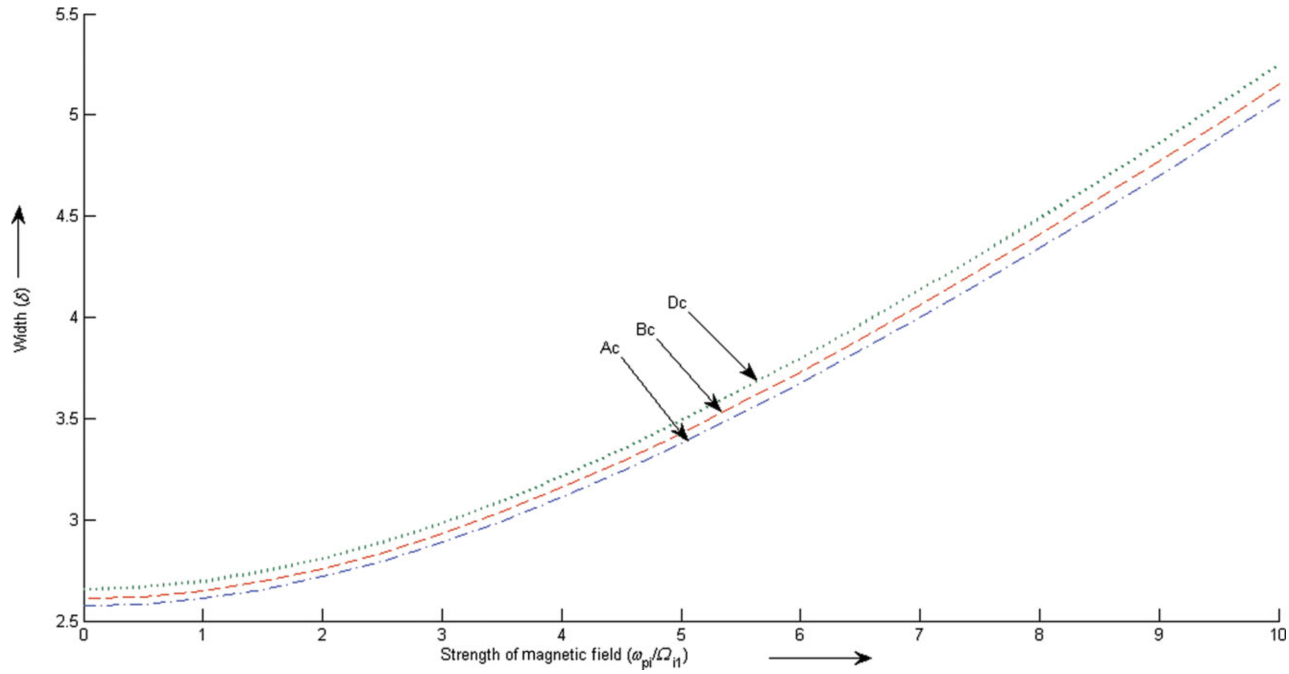

Figure 7. (Colour online) Variation of the slow ion-acoustic soliton width δ with the strength of magnetic field (ω_{pi}/Ω_i) for compressive solitons for (Xe^+, F^-) plasma system with plasma parameters as ($Z_1 = 1, Z_2 = 1$, $\varepsilon_Z = 1$, $\sigma_1 = 0, \sigma_2 = 0.1$, $\alpha = 0.2$, $=$ 5, $u = 0.03$, and $\mu = 6.667$) for three different values of non-thermal parameter ($\gamma = 0$ (shown by dot dashed line), 0.15 (shown by dotted line), and 0.35 (shown by dotted line)).

must be greater than the thermal velocities of ions. We found from numerical calculation that for the (Xe^+, F^-) plasma system with parameter values of $(\sigma_1, \sigma_2) = (0.1, 0.001)$ and α lying in the range of (0.0001−0.012), i.e. in the range of existence of compressive solitons, and (0.04–0.06), i.e. in the range of existence of rarefactive solitons, the ratio of phase velocity to ions thermal velocity lies in the range of (14.36–3.58) and (16.32–4.00). Therefore, our numerical calculation shows that the phase velocity of the fast ion-acoustic mode is much greater than the thermal velocities of ions, hence the wave will not Landau damp. The variation in amplitude of compressive (rarefactive) solitons in different plasma systems with negative ion concentrations is shown in Fig. 8. It may be concluded from the figure that the amplitude of compressive (rarefactive) solitons increases (decreases) with higher μ, i.e. mass of positive ion species is larger as compared to negative ion species. Positive ion due to its inertia will have lower thermal speed as compared with negative ion, therefore the amplitude of rarefactive soliton will decrease; however, it will enhance the amplitude of compressive ion-acoustic solitons. It is interesting to note that for a particular plasma system there exists compressive solitons at lower α with higher μ. Increase in α increases the amplitude of compressive soliton rapidly, as the velocity of the fast mode is a function of α in plasma and should increase with increasing percentage of negative ions (D'Angelo et al. 1966) up to α_c. A compressive soliton steepens due to fluid velocity of positive ions. Electrons follow the steepening due to higher energy and lighter mass than ions. On the other hand, negative ions pull back the steepening due to their larger inertia. At a certain density of negative ions α_c (at critical density) the steepening does not occur, which corresponds to vanishing of the term in the KdV equation. At α_c both compressive and rarefactive solitons coexist. At further increase in negative ion concentration above α_c, there appears rarefactive solitons whose amplitude decreases rapidly with increase in negative ion concentration. It is found that the value of α_c decreases with increase in μ.

It is found from numerical analysis that the nature of soliton depends on negative ion concentration. Figures 9 and 10 show three-dimensional profile for compressive (rarefactive) ion-acoustic solitons in fast mode. We found that amplitude increases (decreases) with an increase in negative ion concentration for the selected range of α. In Fig. 11, we plotted the three-dimensional profile for compressive ion-acoustic solitons in fast mode with non-thermal parameter. It is found that on increasing the values of γ, the amplitude of compressive soliton increases.

Figure 12 shows variation in amplitude with α for four different values of γ. It is found that on increasing α, the amplitude of compressive ion-acoustic soliton increases, on further increasing α the amplitude of compressive soliton increases rapidly up to certain concentration, and on still further increasing α compressive solitons disappear and rarefactive solitons appear with large amplitude, but the amplitude of the rarefactive solitons decreases rapidly with further increase in α. We found that on increasing the values of γ, the amplitude of the

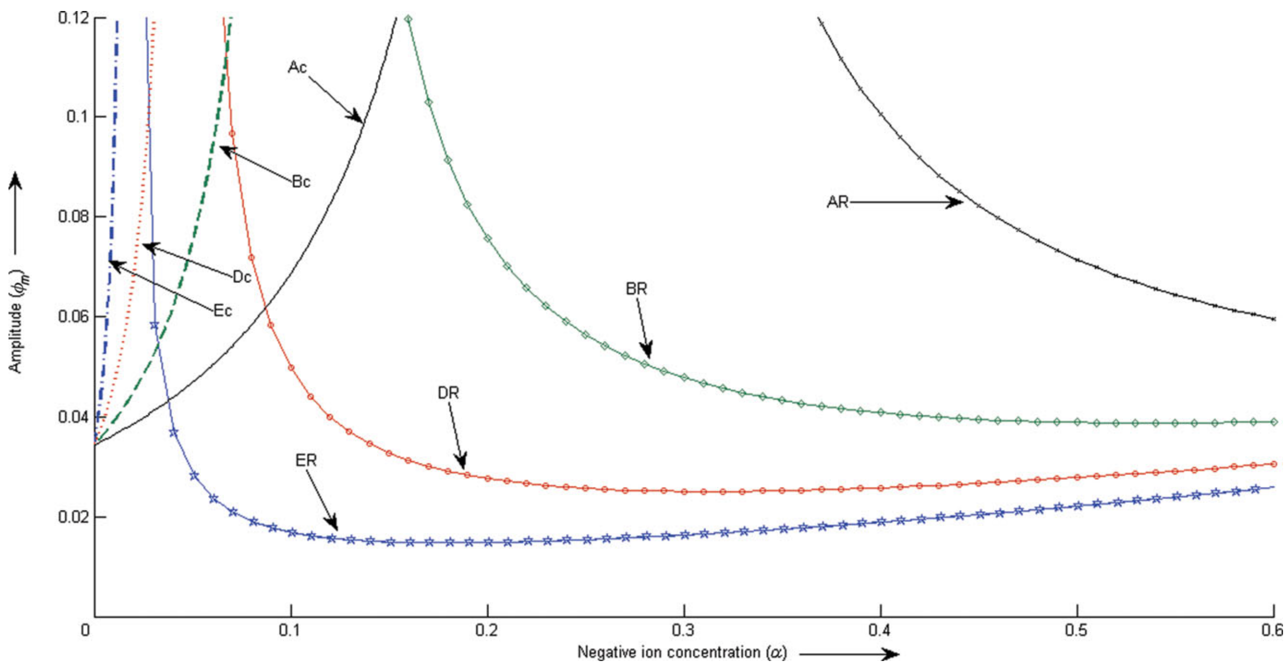

Figure 8. (Colour online) Variation of the fast ion-acoustic soliton amplitude $|\phi_m|$ with negative ion concentration (α) for (H^+, H^-), (Ar^+, F^-), (Cs^+, Cl^-), and (Xe^+, F^-) plasma systems with plasma parameters as ($Z_1 = 1, Z_2 = 1$, $\varepsilon_Z = 1$, $\sigma_1 = 0.1, \sigma_2 = 0, \theta = 15^0$, $\gamma = 0.15$, $(\omega_{pi}/\Omega_i) = 5$, and $u = 0.01$) considering ($\mu = 1.0$ (solid line A_C), 2.1 (dashed line B_C), 3.75 (dotted line D_C), and 6.667 (dot dashed line E_C)) for compressive and rarefactive solitons represented by ($\mu = 1.0$ (solid line with AR), 2.1 (solid line with BR), 3.75 (solid line with DR), and 6.667 (solid line with ER)).

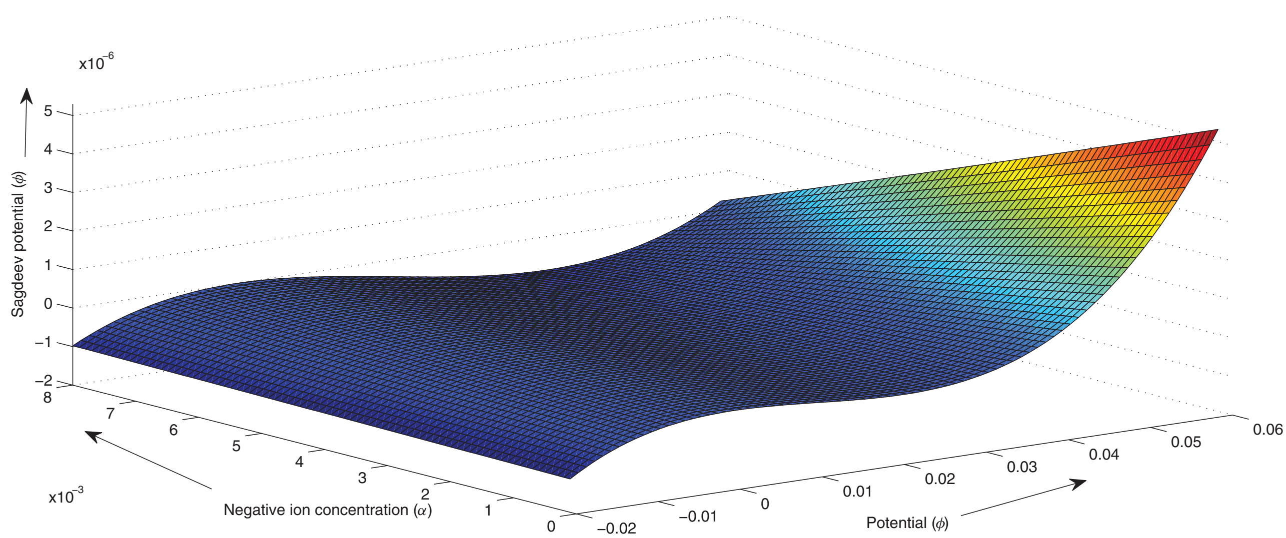

Figure 9. (Colour online) Three-dimensional profile of Sagdeev potential $\psi(\phi)$ with potential ϕ of fast mode compressive ion-acoustic soliton for (Xe^+, F^-) plasma system having $\mu = 6.667$ with negative ion concentration ($\alpha = 0.001$–0.008) with other plasma parameters as ($Z_1 = 1, Z_2 = 1$, $\varepsilon_Z = 1$, $\sigma_1 = 0.1, \sigma_2 = 0.0001, \theta = 15^0$, $(\frac{\omega_{pi}}{\Omega_i}) = 7$, $u = 0.06$, and $\gamma = 0.1$).

compressive soliton increases whereas that of rarefactive soliton decreases. It can be seen from Fig. 9 that an increase in γ decreases the value of α_c.

We have done numerical investigation for finding the effect of strength of magnetic field as well as θ on the amplitude of compressive and rarefactive solitons in fast mode. We found that although strength of magnetic field has no effect on amplitude of compressive and rarefactive solitons, the angle of obliqueness of the wave with magnetic field affects the amplitude of both the solitons. It can be easily seen in Fig. 13 that amplitude of solitons increases slowly for smaller θ, and for higher values of θ, the amplitude of solitons increases rapidly. To find out the effect of non-thermality of energetic electrons, we plotted the curves at three different values of γ. It is found that increase in γ increases (decreases) the amplitude of solitons in case of compressive (rarefactive) solitons.

https://doi.org/10.1017/S0022377813000652 Published online by Cambridge University Press

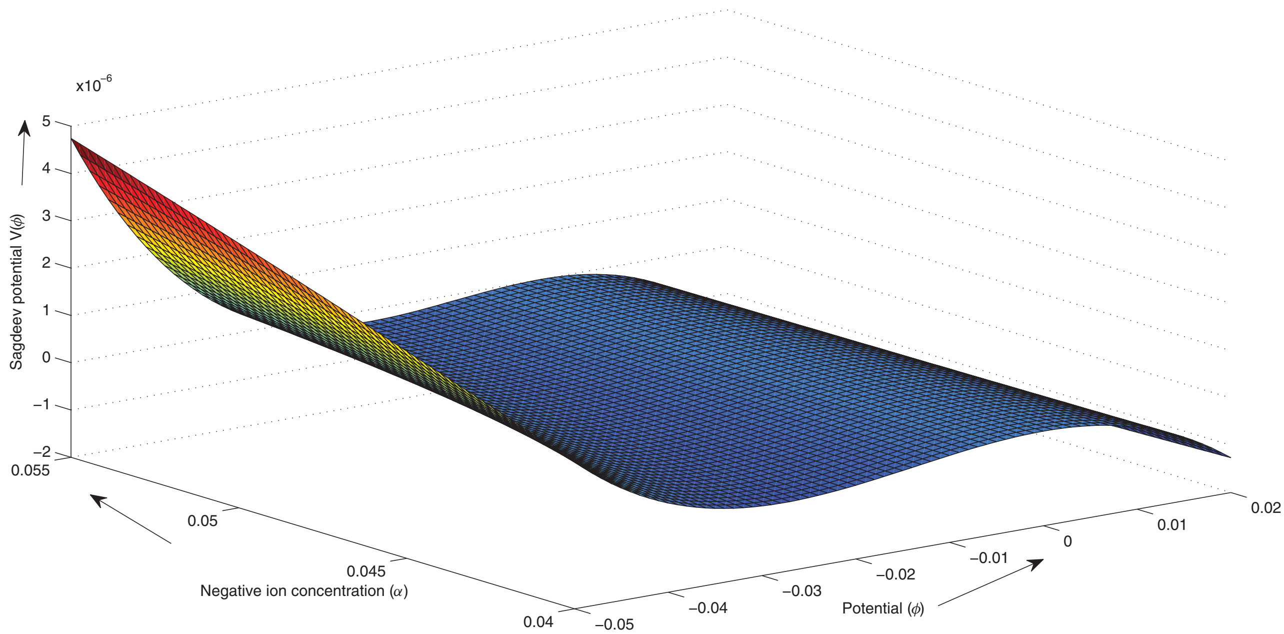

Figure 10. (Colour online) Three-dimensional profile of Sagdeev potential $\psi(\phi)$ with potential ϕ of fast mode rarefactive ion-acoustic soliton for (Xe^{+}, F^{-}) plasma system having $\mu = 6.667$ with negative ion concentration ($\alpha = 0.04$–0.045) with other plasma parameters as ($Z_1 = 1, Z_2 = 1$, $\varepsilon_Z = 1$, $\sigma_1 = 0.1, \sigma_2 = 0.0001, \theta = 15^0$, $(\frac{\omega_{pi}}{\Omega_i}) = 7$, $u = 0.06$, and $\gamma = 0.1$).

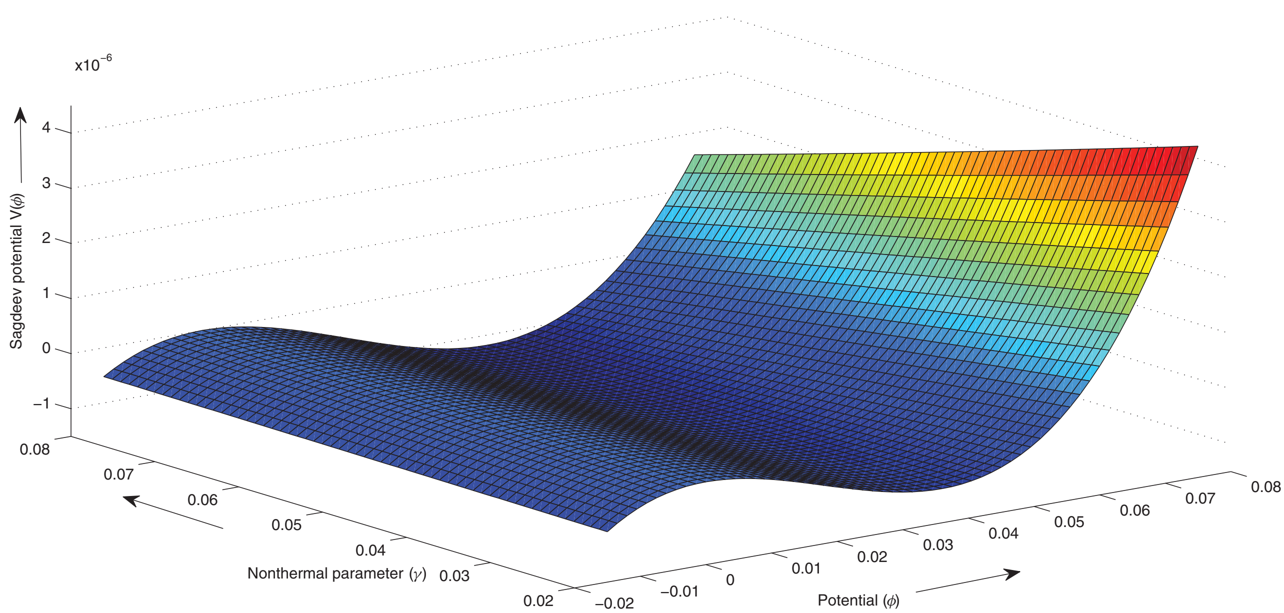

Figure 11. (Colour online) Three-dimensional profile of Sagdeev potential $\psi(\phi)$ with potential ϕ of fast mode compressive ion-acoustic soliton for (Xe^{+},F^{-}) plasma system having $\mu = 6.667$ with non-thermal parameter ($\gamma = 0.02$–0.08) with other plasma parameters as ($Z_1 = 1, Z_2 = 1$, $\varepsilon_Z = 1$, $\sigma_1 = 0.1, \sigma_2 = 0.0001, \theta = 15^0$, $(\frac{\omega_{pi}}{\Omega_i}) = 7$, $u = 0.06$, and $\alpha = 0.01$).

To investigate the effect of strength of magnetic field as well as angle of obliqueness on the width of compressive and rarefactive solitons in fast mode, our results are presented in Figs. 14 and 15. It is found that the width of solitons increases with an increase in θ, reaches at a peak value, and any further increase in θ decreases the width of solitons. It is also found that an increase in γ increases (decreases) the width of compressive (rarefactive) solitons. Figure 15 clearly shows that the width of solitons increases with increase in the strength of magnetic field in compressive and rarefactive solitons. It is also found that with an increase in γ, the width of compressive and rarefactive solitons increases.

For the study of the m-KdV soliton, we numerically evaluated α_c for four plasma systems, namely (H^{+}, H^{-}),

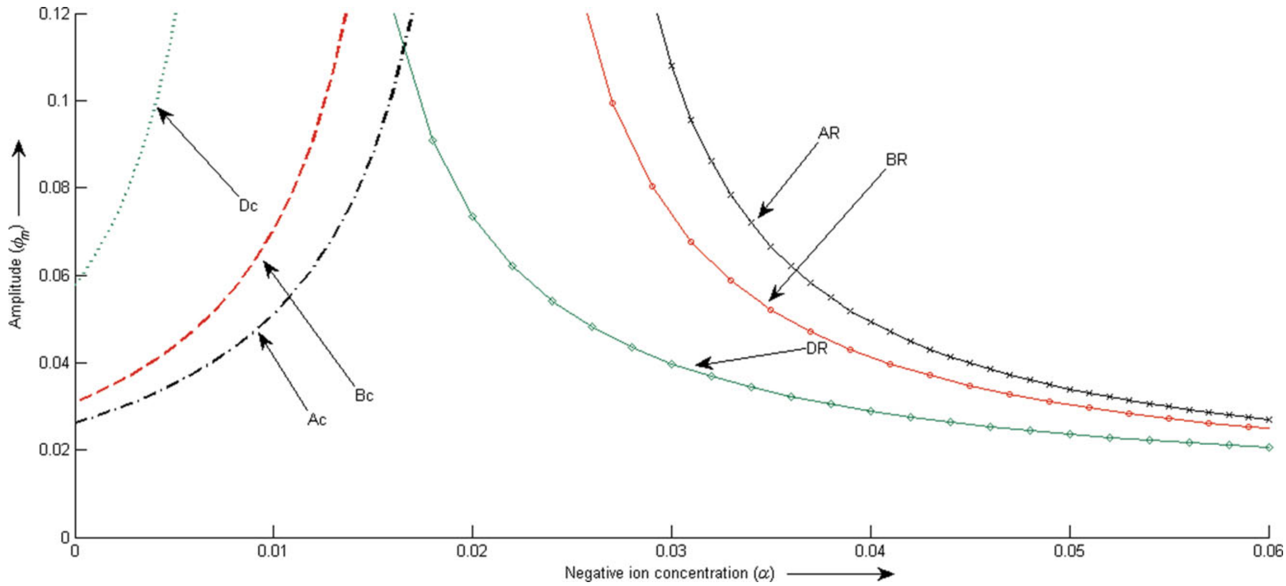

Figure 12. (Colour online) Variation of fast ion-acoustic soliton amplitude $|\phi_m|$ with negative ion concentration (α) for (Xe^+, F^-) plasma system with plasma parameters as ($Z_1 = 1, Z_2 = 1$, $\varepsilon_Z = 1$, $\sigma_1 = 0.1, \sigma_2 = 0.001, \theta = 15^0$, $(\omega_{pi}/\Omega_i) = 5$, $u = 0.02$, and $\mu = 6.667$) for three different values of non-thermal parameters at $\gamma = 0$, 0.15, and 0.3 assigned as A, B, D with C and R corresponding to compressive and rarefactive solitons. Curve A_C shown by dot dashed line, B_C shown by dashed line, and D_C shown by dotted line refer to compressive solitons, and for rarefactive solitons are represented by (solid line with AR), 2.1 (solid line with BR), 3.75 (solid line with DR).

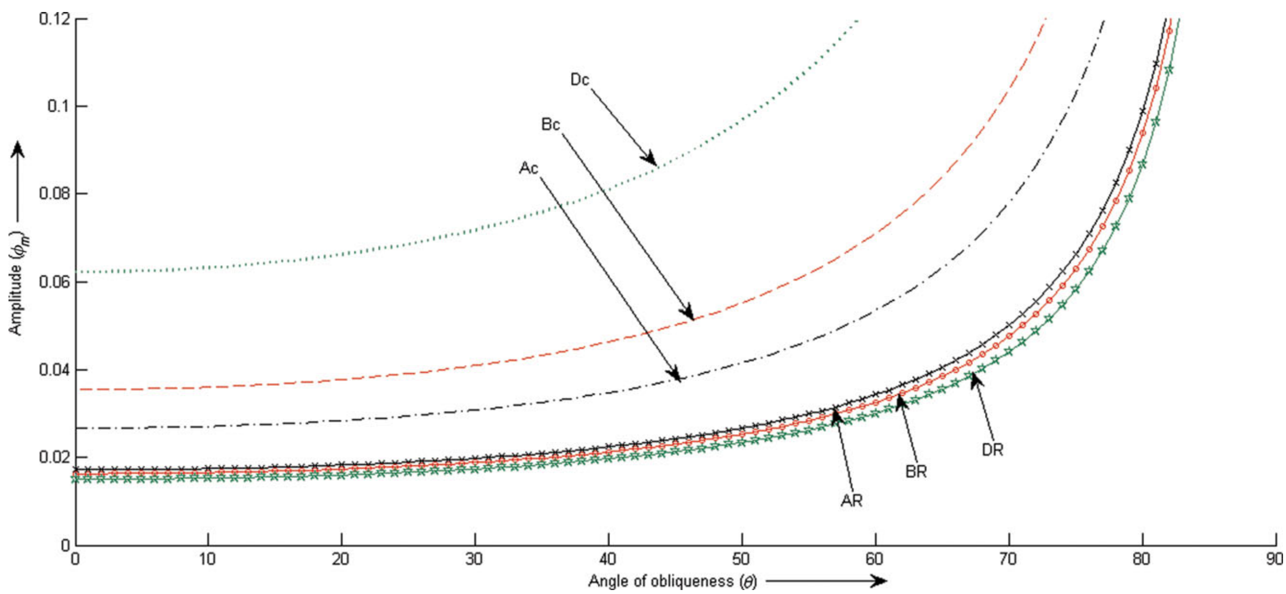

Figure 13. (Colour online) Variation of fast ion-acoustic soliton amplitude $|\phi_m|$ with angle of obliqueness (θ) for (Xe^+, F^-) plasma system with plasma parameters as ($Z_1 = 1, Z_2 = 1$, $\varepsilon_Z = 1$, $\sigma_1 = 0.1, \sigma_2 = 0.0001$, $(\omega_{pi}/\Omega_i) = 5$, $u = 0.01$, and $\mu = 6.667$) for $\alpha = 0.001$ corresponding to compressive and $\alpha = 0.1$ for rarefactive solitons at three different values of non-thermal parameter ($\gamma = 0$ (shown by dot dashed line Ac), (0.15 shown by dotted line Bc), and 0.3 (shown by dotted line Dc) for compressive solitons, and for rarefactive solitons represented by ($\gamma = 0$, solid line with AR), (0.15, solid line with BR), and (0.3, solid line with DR).

(Ar^+, F^-), (Cs^+, Cl^-), and (Xe^+, F^-) at different values of non-thermal parameters. The critical density in a three-component plasma depends upon positive ion to negative ion mass ratio μ, as this ratio increases, α_c diminishes to zero and for smaller values of μ, α_c approaches (2/3) (Cooney et al. 1993). The value of α_c lies well within the range. In Table 1 we have tabulated α_c for the (Xe^+, F^-) plasma system at different values of γ with corresponding amplitude and width of the m-KdV soliton. It can be easily inferred from the table that α_c decreases with increasing γ. It is also to be noted that the amplitude and the width increase with increasing γ. In Table 2, we have tabulated α_c for the (Cs^+, Cl^-) plasma system at different values of γ with corresponding amplitude and width of the m-KdV soliton. It can be easily inferred from the table that α_c

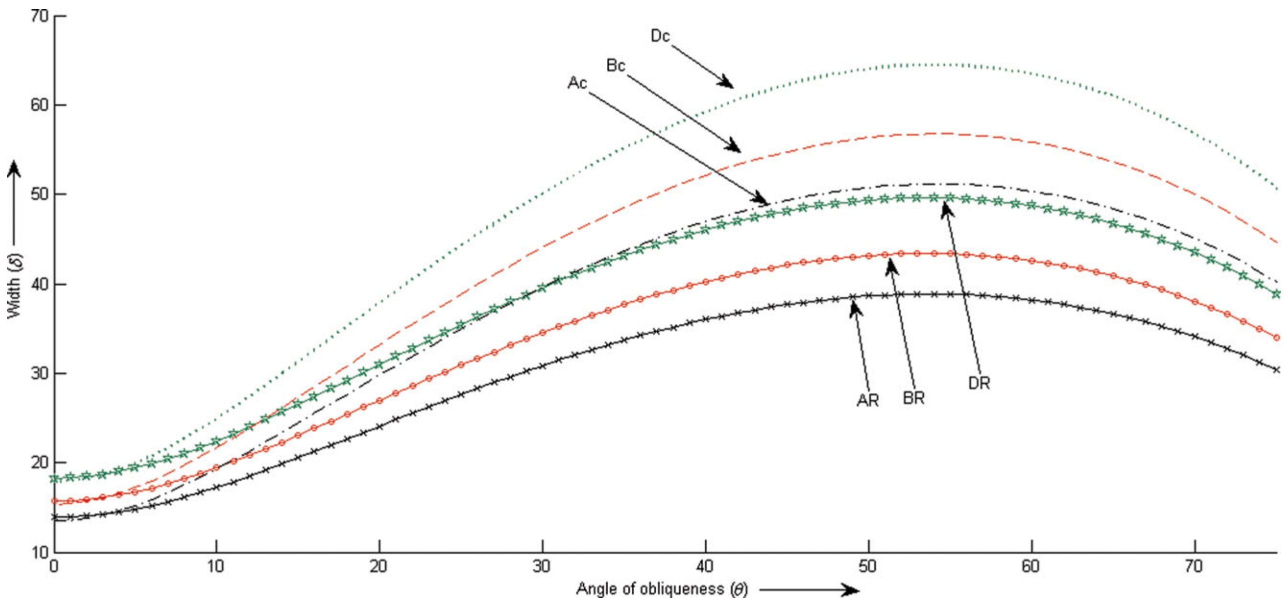

Figure 14. (Colour online) Variation of fast ion-acoustic soliton width δ with angle of obliqueness (θ) for (Xe^+, F^-) plasma system with plasma parameters as ($Z_1 = 1, Z_2 = 1$, $\varepsilon_Z = 1$, $\sigma_1 = 0.1, \sigma_2 = 0.0001, \alpha = 0.2$, $(\omega_{pi}/\Omega_i) = 5$, $u = 0.01$, and $\mu = 6.667$) for $\alpha = 0.001$ corresponding to compressive and $\alpha = 0.1$ for rarefactive solitons at three different values of non-thermal parameter ($\gamma = 0$ shown by dot dashed line Ac), (0.15 shown by dotted line Bc), and (0.3 shown by dotted line Dc) for compressive solitons, and for the rarefactive solitons represented by ($\gamma = 0$, solid line with AR), (0.15, solid line with BR), and (0.3, solid line with DR).

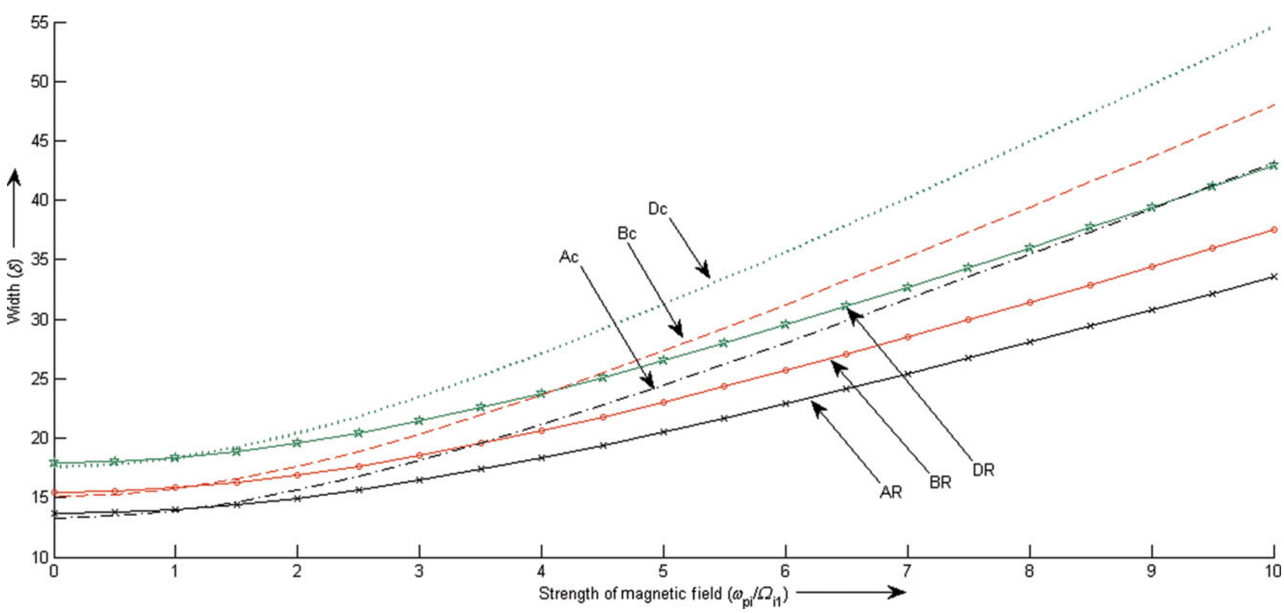

Figure 15. (Colour online) Variation of fast ion-acoustic soliton width δ with the strength of magnetic field (ω_{pi}/Ω_i) for (Xe^+, F^-) plasma system with plasma parameters as ($Z_1 = 1, Z_2 = 1$, $\varepsilon_Z = 1$, $\sigma_1 = 0.1, \sigma_2 = 0.0001, \alpha = 0.2$, $(\omega_{pi}/\Omega_i) = 5$, $u = 0.01$, and $\mu = 6.667$) for $\alpha = 0.001$ corresponding to compressive and $\alpha = 0.1$ for rarefactive solitons at three different values of non-thermal parameter ($\gamma = 0$ shown by dot dashed line Ac), (0.15 shown by dotted line Bc), and (0.3 shown by dotted line Dc) for compressive solitons, and for rarefactive solitons represented by ($\gamma = 0$, solid line with AR), (0.15, solid line with BR), and (0.3, solid line with DR).

decreases with increasing γ. It is also to be noted that the amplitude and the width increase with increasing γ. It is found from the comparison of Tables 1 and 2 that the value of α_c increases with decrease in μ. Our findings of α_c are in accordance as reported by Cooney et al. (1993) in their observation on negative ion plasmas. It is also to be noted that the amplitude of the soliton increases with decrease in μ but its width decreases with decrease in μ. Tables 3 and 4 show similar data for α_c for (Ar^+, F^-) and (H^+, H^-) plasma systems. It is found that α_c strongly depends on the mass ratio of the two ion species. For the plasma having lower values of μ, α_c of negative ions is higher for the existence of m-KdV solitons.

https://doi.org/10.1017/S0022377813000652 Published online by Cambridge University Press

Table 1. Critical negative ion concentration α_c, amplitude, and width with different non-thermal parameter values for (Xe^+, F^-) plasma with $Z_1 = 1$, $Z_2 = 1, \varepsilon_z = 1$, $\sigma_1 = 0.1$, $\sigma_2 = 0.0001$, $\mu = 6.667$, $u = 0.01$, $\theta = 15^0$, and $(\frac{\omega_{pi}}{\Omega_i}) = 5$.

Non-thermal Parameter (γ)	Critical Concentration (α_c)	Amplitude (ϕ_m)	Width (δ)
0	0.02277305464	0.0985	11.6187
0.05	0.021103617448	0.1039	12.0785
0.1	0.019306443515	0.1106	12.5858
0.15	0.01735724576	0.1188	13.1489
0.2	0.01522610392	0.1295	13.7780
0.25	0.01287591565	0.1444	14.4864
0.3	0.0102603633	0.1673	15.2911
0.35	0.00732123174	0.2092	16.2144
0.4	0.00398485493	0.3331	17.2862

Table 2. Critical negative ion concentration α_c, amplitude, and width with different non-thermal parameter values for (Cs^+, Cl^-) plasma with $Z_1 = 1$, $Z_2 = 1$, $\varepsilon_z = 1$, $\sigma_1 = 0.1$, $\sigma_2 = 0.0001$, $\mu = 3.75$, $u = 0.01$, $\theta = 15^0$, and $(\frac{\omega_{pi}}{\Omega_i}) = 5$.

Non-thermal Parameter (γ)	Critical Concentration (α_c)	Amplitude (ϕ_m)	Width (δ)
0	0.06135581320	0.1442	11.3561
0.05	0.05664856317	0.1516	11.8271
0.1	0.05159287701	0.1606	12.3480
0.15	0.04613544925	0.1720	12.9275
0.2	0.04021301201	0.1873	13.5766
0.25	0.03375019221	0.2092	14.3095
0.3	0.02665683764	0.2446	15.1443
0.35	0.01882468729	0.3171	16.1050
0.4	0.01012319895	0.6527	17.2238

Table 3. Critical negative ion concentration α_c, amplitude, and width with different non-thermal parameter values for (Ar^+, F^-) plasma with $Z_1 = 1$, $Z_2 = 1$, $\varepsilon_z = 1$, $\sigma_1 = 0.1$, $\sigma_2 = 0.0001$, $\mu = 2.1$, $u = 0.01$, $\theta = 15^0$, and $(\frac{\omega_{pi}}{\Omega_i}) = 5$.

Non-thermal Parameter (γ)	Critical Concentration (α_c)	Amplitude (ϕ_m)	Width (δ)
0	0.1465786235	0.2239	11.2044
0.05	0.1347326574	0.2340	11.6842
0.1	0.12208145842	0.2468	12.2151
0.15	0.1085310072	0.2639	12.8061
0.2	0.09397297725	0.2880	13.4685
0.25	0.07828206824	0.3257	14.2167
0.3	0.06131268409	0.3953	15.0693
0.35	0.04289480733	0.5923	16. 0508

Table 4. Critical negative ion concentration (α_c), amplitude, and width with different non-thermal parameter values for (H^+, H^-) plasma with $Z_1 = 1$, $Z_2 = 1$, $\varepsilon_z = 1$, $\sigma_1 = 0.1$, $\sigma_2 = 0.0001$, $\mu = 1$, $u = 0.01$, $\theta = 15^0$, and $(\frac{\omega_{pi}}{\Omega_i}) = 5$.

Non-thermal Parameter (γ)	Critical Concentration (α_c)	Amplitude (ϕ_m)	Width (δ)
0	0.32786050071	0.4278	11.7034
0.05	0.30148675366	0.4496	12.1721
0.1	0.27324294641	0.4808	12.6869
0.15	0.24292980280	0.5292	13.2556
0.2	0.21031898470	0.6141	13.8874
0.25	0.17514761057	0.8099	14.5942

6. Conclusions

Our main findings in negative magnetized plasma with non-thermal electrons are as follows:

1. Due to consideration of different finite ion temperatures of two species there exist two modes of propagation in the plasma having negative and positive ions, namely slow and fast ion acoustic modes.
2. In the case of slow ion-acoustic mode, relative ratio of ion temperature to mass of ion species is the relevant parameter for determining the nature of solitons (i.e. compressive or rarefactive). If the ratio of temperature of positive ion species to μ is less than the temperature ratio of negative ion species (i.e. $(\sigma_1/\mu < \sigma_2)$), then compressive solitons exist; if $(\sigma_1/\mu > \sigma_2)$, then only rarefactive solitons exist.
3. In the case of slow ion-acoustic mode, it is found that on increasing the value of γ the amplitude of compressive (rarefactive) soliton decreases (increases). The amplitude of solitons also increases with increase in α.
4. In case of fast ion-acoustic mode, it is found that the nature of solitons depends on α in the plasma system. For the selected set of plasma parameters, the compressive solitons exist at relatively lower values of α with higher values of μ. The amplitude of compressive solitons increases with increase in the value of α, on further increasing the value of α, the amplitude of compressive solitons increases sharply. On further enhancement in α, the nature of solitons changes from compressive to rarefactive with large amplitude, but amplitude decreases sharply with further increase in the value of α. Therefore, there must be a value of α at which both compressive and rarefactive solitons coexist. The value of α at which both compressive and rarefactive solitons coexist is known as critical value of negative ion concentration (α_c).
5. In the case of both slow and fast modes, the amplitude of compressive (rarefactive) soliton increases (decreases) with increasing μ for the selected set of parameters.
6. In the case of fast mode, the amplitude of compressive (rarefactive) soliton increases (decreases) with increase in γ.
7. The value of α_c decreases with increase in μ. An increase in non-thermal parameter also decreases the value of α_c for a selected set of plasma parameters.
8. The amplitude and width of the m-KdV soliton increase with increase in μ; an increase in γ also increases the amplitude and width of the m-KdV soliton.

The investigation should be helpful in understanding the salient features of nonlinear ion-acoustic solitary structures observed in the laboratory and space where two distinct groups of ions and non-thermal electrons are present.

Acknowledgments

One of the authors (S. K. Jain) thankfully acknowledges the U.G.C., Govt. of India, for providing Teacher Research Fellowship to complete the research work.

References

Asbridge, J. R., Bame, S. J. and Strong, I. B. 1968 *J. Geophy. Res.* **73**, 5777.

Bacal, M. and Hamilton, G. W. 1979 *Phys. Rev. Lett.* **42**, 1538.

Barman, S. N., and Talukdar, A. 2010 *Int. J. Appl. Math. Mech.* **6**, 47.

Cairns, R. A., Mamun, A. A., Bingham, R., Bostrom, R., Dendy, R. O., Nairn, C. M. C. and Shukla, P. K. 1995 *Geophys. Res. Lett.* **22**, 2709.

Cairns, R. A., Mamun, A. A., Bingham, R., and Shukla, P. K. 1996 *Phys. Scripta* **T63**, 80.

Chaizy, P. H., Reme, H., Sauvayd, J. A., D'uston, C., Lin, R. P., Larson, D. E., Mitchell, D. L., Anderson, K. A., Carlson, C. W., Korth, A., et al. 1991 *Nature* (London) **349**, 393.

Coates, A. J., Crary, F. J., Lewis, G. R., Young, D. T., Waite Jr., J. H. and Sittler, E. C. 2007 *Geophys. Res. Lett.* **34**, L22103.

Cooney, J. L., Aossey, D. W., Williamst, J. E., Gavin, M. T., Kim, H. S., Hsu, Y. C., Scheller, A. and Lonngren, K. E. 1993 *Plasma Sources Sci. Technol.* **2**, 73.

Cooney, J. L., Gavin, M. T. and Lonngren, K. E. 1991 *Phys. Fluids* **B3**(10), 2758.

D'Angelo, N., Von Goeler, S. and Ohe, T. 1966 *Phys. Fluids* **9**, 1605.

Das, G. C. and. Tagare, S. G. 1975 *Plasma Phys.* **17**, 1025.

Dovner, P. O., Eriksson, A. I., Bostrom, R. and Holback, B. 1994 *Geophys. Res. Lett.* **21**, 1827.

Dudik, J., Dzifcakowa, E., Karlicky, M. and Kulinova, A. 2011 *Astron. Astrophys.* **529**, A103.

El-Labany, S. K., El-Warranki S. A. and Moslem, W. M. 2000 *J. pPlasma Phys.* **63**, 343.

El-Labany, S. K., Sabry, R., El-Taibany, W. F. and Elghmaz, E. A. 2010 *Plasma Phys.* **17**, 042301.

El-Taibany, W. F. and Tribeche, M. 2012 *Plasma Phys.* **19**, 024507.

Gill, T. S., Bala, P., Kaur, H., Saini, N. S., Bansal, S. and Kaur, J. 2004 *Eur. Phys. J.* D **31**, 91.

Gottscho, R. A. and Gaebe, C. E. 1986 *IEEE Trans. Plasma Sci.* **14**, 92.

Hall, D. S., Chaloner, C. P., Bryant, D. A., Lepine, D. R. and Trikakis, V. P. 1991 *J. Geophys. Res.* **96**, 7869.

Ichiki, R., Shindo, M., Yoshimura, S., Watanbe, T. and Kawai, Y. 2001 *Phys. Plasmas* **8**, 4275.

Ichiki, R., Yoshimura, S., Watanbe, T., Nakamura Y. and Kawai, Y. 2002 *Phys. Plasmas* **9**, 4481.

Ikezi, H., Taylor, R. J. and Baker, D. R. 1970 *Phys. Rev. Lett.* **25**, 11.

Islam, Sk. A., Bandopadhyay, A., and Das, K. P. 2009 *Phys. Plasmas* **16**, 022307.

Liberman, M. A. and Lichtenberg, A. J. 2005 *Principles of Plasma Discharges and Materials Processing*, 2nd edn. New York, NY: Wiley.

Ludwig, G. O., Ferreira, J. L. and Nakamura, Y. 1984 *Phys. Rev. Lett.* **52**, 275.

Lundin, R., Eliasson, L., Hultqvist, B. and Stasiewicz, K. 1987 *Geophy. Res. Lett.* **14**, 443.

Lundin, R., Zakharov, A., Pellinen, R., Borg, H., Hultqvist, B., Pissarenko, N., Dubinin, E. M., Barabash, S. W., Liede, I. and Koskimen, H. 1989 *Nature* (London) **341**, 609.

Massey, H. 1976 *Negative Ions*, 3rd edn. Cambridge, UK: Cambridge University Press, 663 pp.

Mishra, M. K., Chhabra, R. S. and Sharma, S. R. 1994 *J. Plasma Phys.* **52**, 409.

Nakamura, Y., Odagiri, T. and Tsukabayashi, I. 2001 *Plasma Phys. Control. Fusion* **39**, 115004.

Nakamura, Y. and Tsukabayashi, I. 1984 *Phys. Rev. Lett.* **52**, 2356.

Pillay, S. R. and Verheest F. 2005 *J. Plasma Phys.* **71**, 177.

Portnyagain, Yu. I., Klyuev, O. F., Shidlovsky, A. A., Evdokimov, A. N., Buzdigar, T. W., Matukhin, P. G., Pasynkov, S. G., Shamshev, K. N., Sokolov, V. V. and Semkin, N. D. 1991 *Adv. Space Res.* **11**, 89.

Rizzato, F. B., Schneider R. S. and Dillenburg, D. 1987 *Plasma Phys. Control. Fusion* **29**, 1127.

Sabry, R., Moslem, W. M. and Shukla, P. K. 2009 *Plasma Phys.* **16**, 032302.

Saito, M., Watanbe, S. and Tanaka, H. 1984 *J. Phys. Soc. Jpn.* **53**, 2304.

Stverak, S., Maksimovic, M., Travenicek, P. M., Marsch, E., Fazakerley, A. N. and Scime, E. E. 2009 *J. Geophys. Res.* **114**, A05104. doi:10.1029/2008JA013883.

Swider, W. 1988 *Ionosphere Modelling* (ed. J. N. Korenkov). Berlin 14197 Germany: Birkhauser Basel, 403 pp.

Tagare, S. G. and Reddy, R. V. 1987 *Plasma Phys. Control. Fusion* **29**, 671.

Washimi, H. and Taniuti, T. 1966 *Phys. Rev. Lett.* **17**, 996.

Watanabe, S. 1984 *J. Phys. Soc. Jpn.* **53**, 952.

Yadav, L. L. and Sharma, S. R. 1990 *Phys. Lett.* A **150**, 397.